In presenting the dissertation as a partial fulfillment of the requirements for an advanced degree from the Georgia Institute of Technology, I agree that the Library of the Institution shall make it available for inspection and circulation in accordance with its regulations governing materials of this type. I agree that permission to copy from, or to publish from, this dissertation may be granted by the professor under whose direction it was written, or, in his absence, by the dean of the Graduate Division when such copying or publication is solely for scholarly purposes and does not involve potential financial gain. It is understood that any copying from, or publication of, this dissertation which involves potential financial gain will not be allowed without written permission.

Don Charles Banks

A STUDY OF BEARING CAPACITY IN SANDS UNDER DYNAMIC LOADING

A THESIS

Presented to

the Faculty of the Graduate Division

by

Don Charles Banks

In Partial Fulfillment

of the Requirements for the Degree

Master of Science in Civil Engineering

Georgia Institute of Technology

April, 1963

5A
12T

A STUDY OF BEARING CAPACITY IN SANDS UNDER DYNAMIC LOADING

Approved:

Date Approved by Chairman: April 16, 1963

ACKNOWLEDGMENTS

To Dr. Aleksander B. Vesic, for his suggestion of this research and for his direction and aid in conducting the investigation and preparation of this text, the author is most appreciative. The comments on the text by Professors George F. Sowers and Charles E. Stoneking were very beneficial to its preparation.

TABLE OF CONTENTS

LIST OF TABLES

LIST OF ILLUSTRATIONS

Figure Page

SUMMARY

The object of this investigation was to study the influence of the rate of loading on the bearing capacity of a shallow footing on a sand.

Model tests were performed on a 4-inch circular plate resting on the surface of a dense sand. Different rates of loading under strain-controlled conditions were used. The range in load rates varied from 0.93 inches per second to 0.00005 inches per second. Continuous records of the settlement and loads were obtained by a Sanborn Recorder. A small static cone penetrometer provided checks on the density and homogeneity of each model.

The tests show an increase in the bearing capacity with an increase in the load rate in the range of load rates used in the study. (In triaxial studies by Whitman and Casagrande and Shannon, an increase in the load at failure was also noted with an increase in the load rate in the same range of rates reported here.) Tests conducted at extremely low load rates were not directly comparable to those tests conducted at the fast rates due to the nonascertainable effects of the loading system upon the test results in the low load range.

There is some evidence that the type of failure at the high rates of loading differs from the type of failure at the low rates of loading. At the low rates of loading an increase in the resistance to penetration of the footing after failure had occurred was noted.

Due to the scattering of results, additional tests should be performed to better determine the phenomena associated with increased load rates.

CHAPTER I

INTRODUCTION

In the past few years several investigations have been made in the field of soil dynamics, both analytically and experimentally. Most of these investigations, however, were concerned with soil behavior under vibratory loading conditions. Very little has been published concerning soil behavior under dynamic, nonvibratory loads. Now, with increased demand for foundations designed to resist a single dynamic load, such as those loads resulting from blasts, there is a corresponding increase in the need for studying soil behavior under such loading conditions.

Among the earliest work done in this area of study was that of Casagrande and Shannon (1) and Whitman (2, 3). Both these studies were concerned with the behavior of triaxial samples under transient (short-termed) loading conditions. Both studies included a variety of soil materials, including sand. Casagrande and Shannon, by varying the time to failure from 2000 seconds to 0.02 seconds reported, in spite of considerable scattering, an increase in the failure load by approximately 15 per cent. They also reported a slight increase of the modulus of deformation with an increase in the load rate. Whitman has stated that there exists a 10 to 15 per cent increase in the strength of a triaxial sample as the strain-rate is increased from that in "the normal slow test" to that in a test completed in a few hundredths of a second. However, De Beer and Vesic (4) found in tests of 2-inch by 12-inch rectangular footings in sand a decrease of the bearing capacity at increased rates of loading.

Some other results of bearing capacity tests with small footings have been published (5, 6, 7, 8). Moreover, it is reported that work is now being performed at the Naval Civil Engineering Laboratory, the University of Illinois, and the Waterways Experiment Station in regard to non-vibratory dynamic loads (9). However, at the present time, there is still not reliable information on the phenomena associated with the bearing capacity of a footing subjected to varying load rates.

In this investigation the author has studied the influence of variations of the rate of loading upon the bearing capacity of a 4-inch circular plate at the surface of a dense sand. The range in load rates varies from approximately 0.00005 inches per second to approximately 0.9 inches per second. This corresponds to times to failure of approximately 5000 seconds to 0.6 seconds, respectively. In all tests a continuous account of the load-time relationship and the settlement-time relationship was recorded.

CHAPTER II

EQUIPMENT AND PROCEDURE

Construction of Models

In the following discussion, the term model includes the footing and the sand used to support the footing. Construction of a model includes placing the sand and the footing. All models, except one, were built by the same procedure in an attempt to gain as much homogeneity as possible, with respect to density, both within a model as well as between all models. The method used in construction of models was vibratory compaction with the exception of the one model constructed by allowing the sand to fall freely from a predetermined height.

Equipment

The following equipment was used in the model construction:

(1) a dry sand,

(2) a box in which the model was built,

(3) a container to deliver the sand to the model box,

(4) a set of vibrator plates, and

(5) a footing.

In the model built by free falling sand, the fourth item was replaced with a set of funnels to deposit the sand uniformly over the surface of the model.

Sand

The models were all constructed with an air-dry, sieved sand obtained from the Chattahoochee River. Drying was accomplished by charging a rotary cement mixer with wet sand and heating over a butane flame. The water content during testing varied from 0.30 per cent to 0.15 per cent. A window screen, with openings slightly greater than a standard number 16 sieve, was used in the sieving process. The resulting grain-size distribution is shown in Figure 1. This sand may be described as a medium, uniform, subangular micaceous sand. Minimum density was 79.0 lb/ft^3, maximum density was 102.5 lb/ft^3.

Preceding this study several triaxial tests had been performed on this sand at densities of 84, 90, 95, and 98 lb/ft^3 with confining pressures of 5, 10, 20, 40, and 80 lb/in^2 for each density. The results of the triaxial tests are shown in Figure 2 (10). As indicated, the angle of internal friction, ϕ , is shown as a function of the void ratio, e .

Model Box

A steel box, 70 inches deep and 50 inches square, was used to contain the model. Lines were constructed at 1-inch increments on the inside of the box so layer thicknesses could be easily determined. The model box is shown in Figures 3 and 4.

Delivery Box

A steel box 2 feet square and 2 feet deep, sloping to a 6 inch opening, was used to elevate the sand and deliver it to the model. The opening was equipped with a manual valve so that the flow of sand could be regulated in obtaining the correct layer thickness.

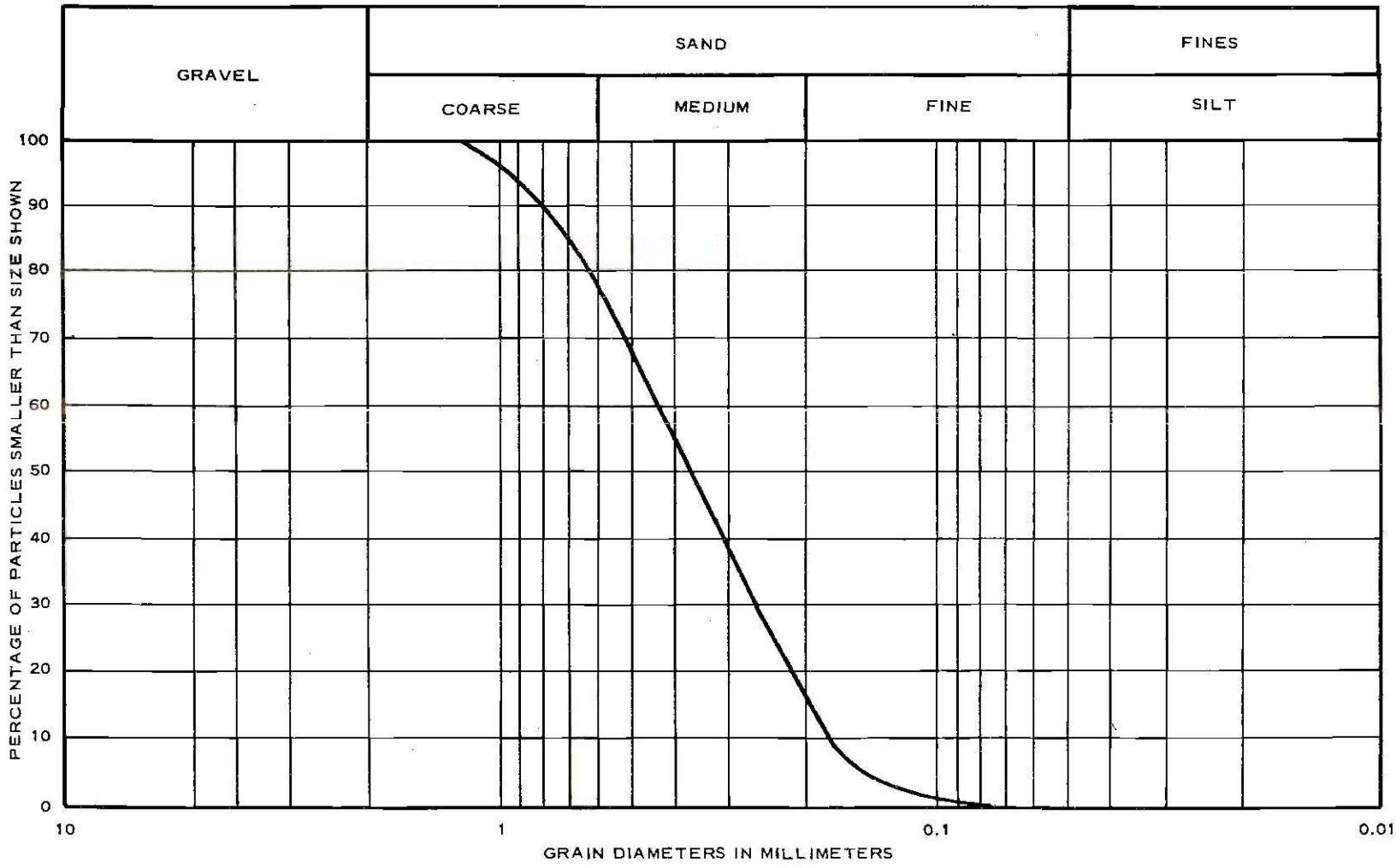

Figure 1. Grain-Size Distribution Curve.

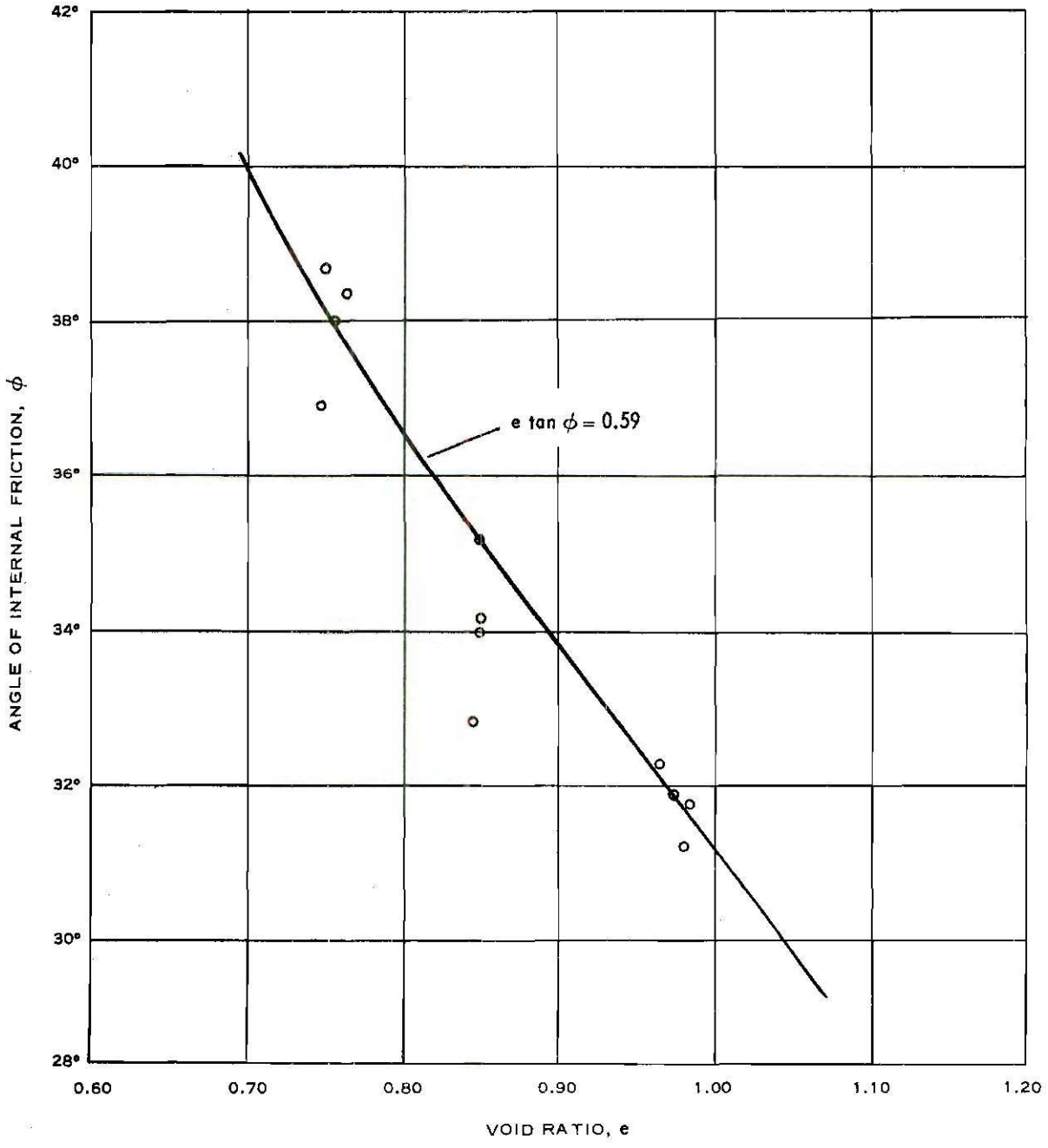

Figure 2. Angle of Internal Friction as a Function of Void Ratio.

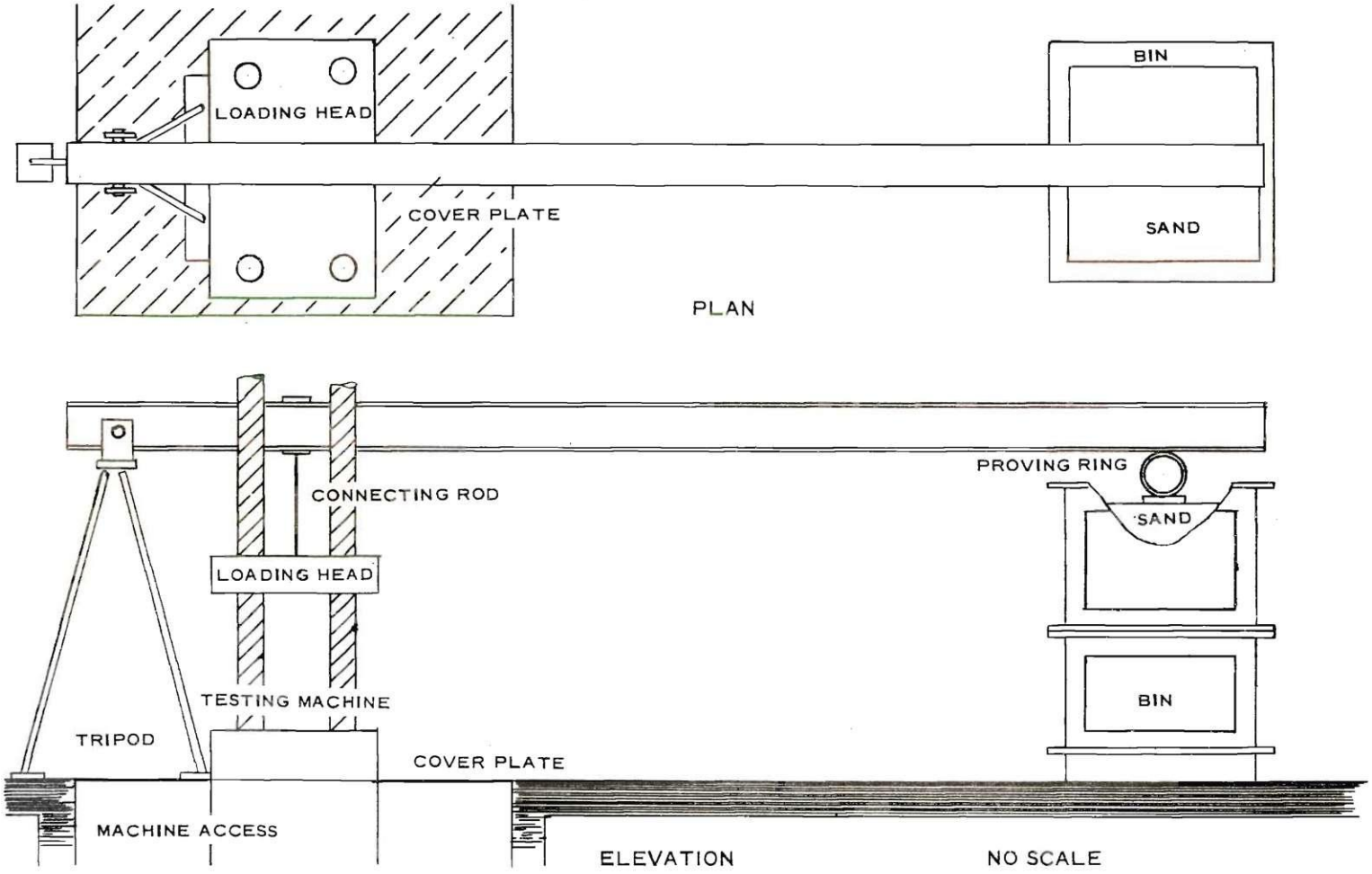

Figure 3. Test Arrangement (Position A).

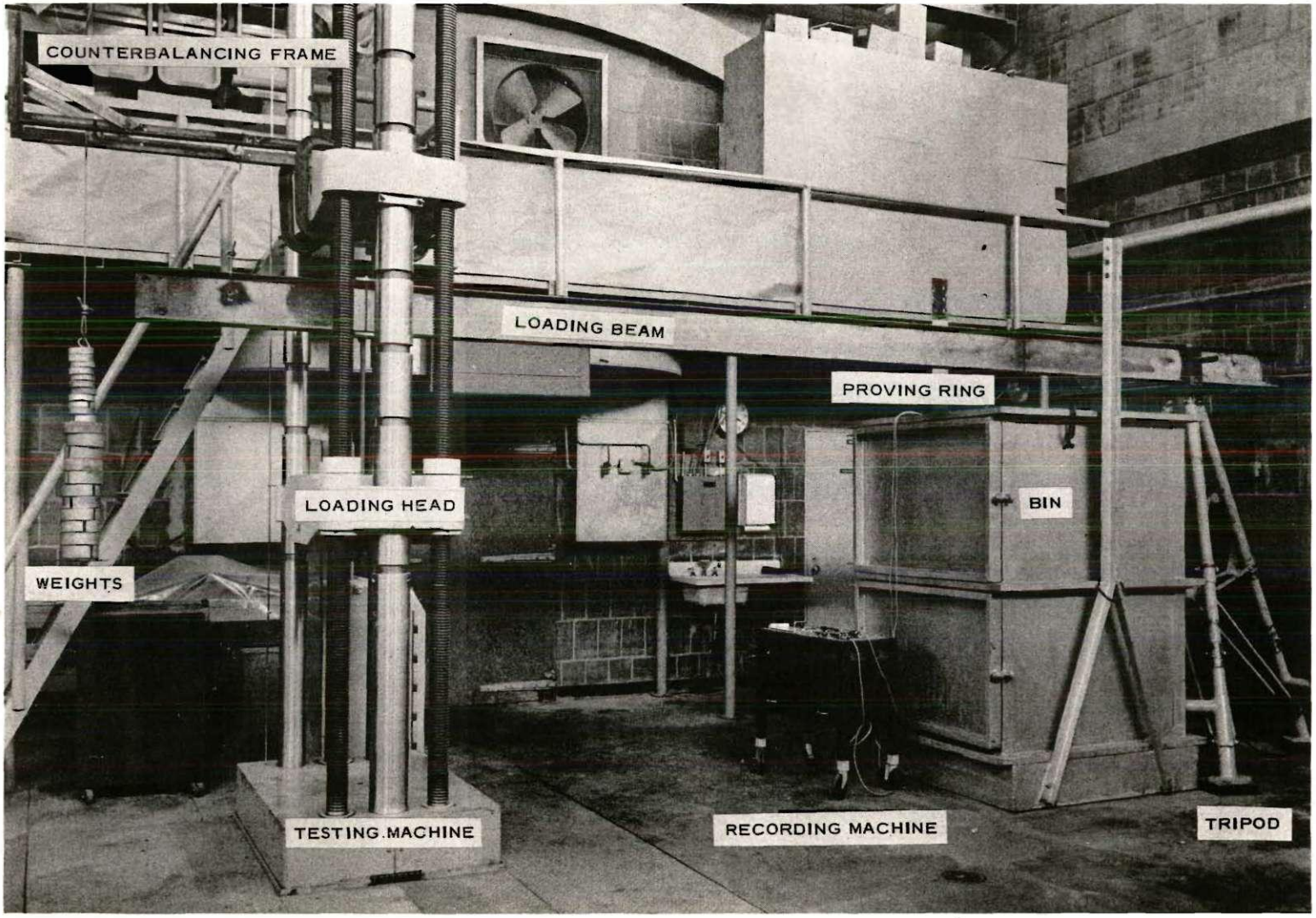

Figure 4. Photograph. Test Arrangement (Position B).

Vibrator Plates

A Syntron Electric Vibrator was attached at the centers of both 24-inch by 48-inch, 1/4-inch thick steel plates. The vibrators had a frequency of 3600 cycles per minute and an amplitude of about 1/32 inch. The weight of the plate and vibrator was 120 pounds. See Figure 5.

Footing

A circular steel plate 1/2-inch thick and 4 inches in diameter served as the footing. To provide a rough interface between the footing and the sand, a sheet of coarse sandpaper was trimmed to the size and shape of the footing and glued to the bottom side. At the center of the top side, a small depression was made to provide a seat for the loading mechanism.

Funnels and Storage Container

In the one model built by allowing the sand to fall freely, the steel delivery box was replaced by a 55-gallon steel drum. Beneath the drum, two openings were provided for 2 1/2-inch rubber hoses. To regulate the flow of sand to the funnels, manual valves were inserted at the midheight of the hoses. The funnels were 6 inches wide by 13 inches and 23 inches in length, tapering inward for 12 inches, in pyramid fashion, to fit the hoses.

Method of Construction

After completing a test, the sand was removed to a depth of approximately 20 inches (five footing diameters) from the surface. The removed sand was stored in steel drums. Any sand spilling was resieved before using again.

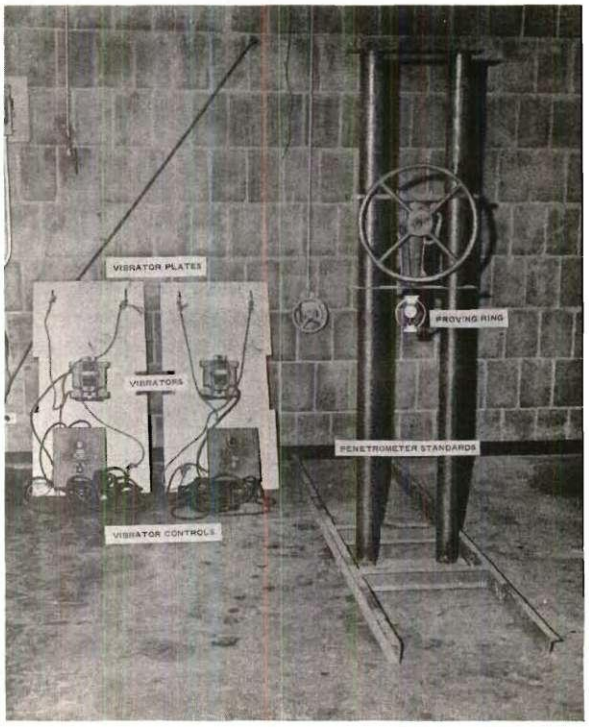

Figure 5. Photograph. Penetrometer and Vibrator Plates.

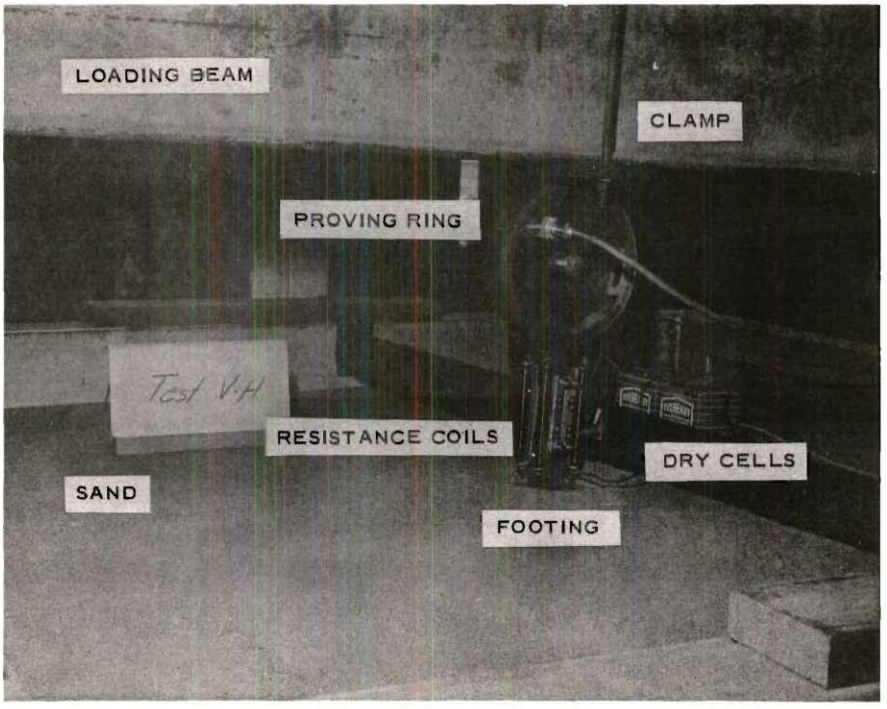

Figure 6. Photograph. Test in Progress.

The surface was smoothed and leveled, then subjected to three minutes of vibration before continuing with construction.

The depth of 20 inches was considered sufficient to escape the effects of the bearing failure of the previous test. The three-minute vibration period was chosen on the basis of previous experiences. It did restore the sand surface, disturbed by the digging and smoothing operation, to a condition homogeneous to the mass.

Four inches of sand was deposited on the surface in a random pattern. The markings on the box were used for the purpose of determining when this four inches was obtained. The leveled and smoothed surface of the four inch layer was then vibrated for three minutes. During vibration the plates were held together and slid over the surface to prevent the formation of a zone of loose material between the two plates. The plates were rotated 90 degrees with each subsequent layer to assure as much as possible that the mass of each model would be close to an average condition.

After the surface of the last layer had been compacted, no other surface preparation was performed for fear of destroying the homogeneity of the model immediately beneath the footing.

There were several possibilities for variation in the manner of construction of a model. For instance, the layer thickness, density of layer before vibration, time of vibration, and surcharge were possible variables. However, it was found that the models could be built with a reasonable effort in the manner described above.

One attempt was made to obtain a lower density with the same confidence of gaining homogeneity within a model and being able to repeat

the density in subsequent models as with the vibratory construction method.

The method used for this construction differed from the previously described method in the manner of placing the sand. The sand was allowed to fall freely from funnels positioned 31 inches from the initial surface. Two-inch layers were deposited before raising the funnel height again to 31 inches. The 13-inch funnel was used to place the sand in a strip near the sides and the 23-inch funnel was used to place the sand in the middle strip. Before placing the footing in its loading position the surface was leveled by scraping with a cutting edge.

Testing

The term testing includes arranging the test equipment, loading the footing, and determining the density of each model. Two arrangements for loading the footing were used. Figures 3 and 4 indicate the beam-tripod positions.

Equipment

The following equipment was used in testing a model:

(1) a pair of resistance coils,

(2) a proving ring,

(3) a recording device,

(4) an arrangement for applying the load, and

(5) a device for determining the density of a model.

The equipment described below was used in all the tests. The only variation in testing was in the fourth item, the arrangement for applying

the load.

Resistance Coils

A pair of resistance coils wired in parallel was attached to each side of the loading column. Each coil had a resistance of 120 ohms varying linearly over its 4-inch length. Two 9-volt dry cell batteries provided the drop in potential across the coils.

A bracket-shaped sliding contact was prepared so that the voltage drop from the bottom of the pair of coils to the contacts could be recorded and related to the deflection of the footing. See Figure 6.

Proving Ring

A proving ring was constructed using four SR-4 strain gages, wired in a Wheatstone Bridge circuit. The mean diameter of the proving ring was 6.1 inches, the thickness was 0.6 inches, and the width was 1.0 inches. The proving ring showed a linear load-strain relationship up to the designed load of 3000 pounds (11).

Holes were tapped top and bottom on the vertical diameter to rigidly attach the proving ring between the loading beam clamp and the loading column. See Figure 6.

Recording Device

A Sanborn Two Channel Recording Instrument, Model #60, was used for recording the load and deflection during the testing operation. This particular model was equipped with a timing device which marked on the recording paper the lapsed time, providing a convenient method of determining the load rate and time to failure.

A Sanborn DC General Purpose Amplifier, Model #64-300B, was used to amplify the voltage change in the resistance coils. Calibration

showed a linear relationship between stylus deflection and the voltage changes. See Figure 7. Through the sensitivity chosen, the settlement was read directly to 0.07 inches and estimated to 0.007 inches.

A Sanborn Strain Gage Amplifier, Model #64-500B, was used to record the strain in the proving ring. Calibration showed that the stylus deflection was not proportioned to the load for the lower load valves and was particularly sensitive to the zeroing position of the stylus. Therefore, it was necessary to check the calibration after every other test. See Figure 8. Through the sensitivity chosen, the load was read directly to 11.1 lb. and estimated to 1.1 lb.

Loading Arrangement

In the first arrangement, Figure 3, the loading beam was pivoted behind the testing machine and was counterweighted behind the model box so that the footing received no load from the dead weight of the loading beam. In this arrangement the rate of movement of the loading head of the testing machine was increased by the lever system. A pivot was constructed so that the loading beam could move down to load the footing.

A load was applied to the footing by allowing the loading head on the testing machine to bear against a bearing plate. The load was then transferred to the loading beam through a threaded rod and beam clamp similar to the one holding the proving ring.

The Riehle Testing Machine is a screw type machine driven by a belt drive. The loading head velocity varies from approximately 0.015 inches per minute in the "Load" range to 20 inches per minute in the "Adjust" range.

In the second arrangement, Figure 4, the equipment is the same.

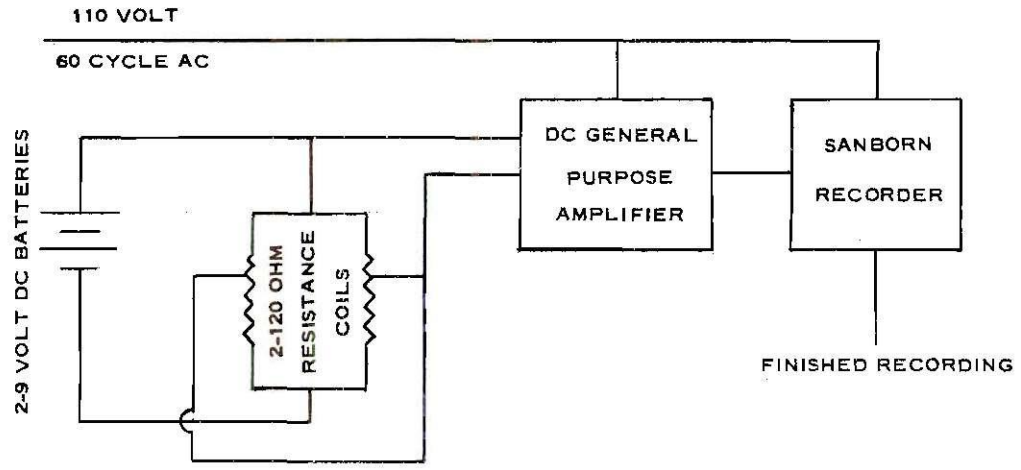

Figure 7. Basic Circuit for Measurement of Deflection.

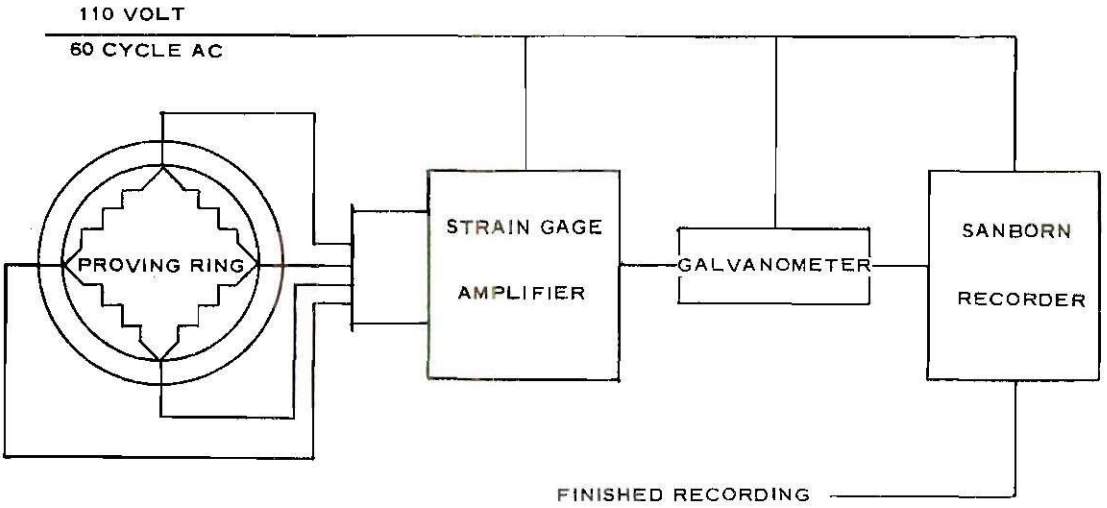

Figure 8. Basic Circuit for Measurement of Load.

The only difference is that the tripod position was reversed with respect to the loading machine so that now the rate of movement of the loading head is reduced by the lever arrangement.

Density Determination

A static cone penetrometer, using a 3/8-inch diameter rod with a 1/2-inch point, was employed to measure the density of each model. See Figure 5.

After a footing had been loaded to failure, two soundings were made. Advancement of the penetrometer rod into the model was in 1-inch increments by the use of a screw jack. The mean of the resistance encountered by the penetrometer, as evidenced by the proving ring, was recorded.

Using Figure 9, a previously determined depth-penetrometer resistance-density relationship for this sand and this penetrometer, the average resistance of the two soundings was reduced to density. Determined at each whole inch, the average density for the first 12 inches was taken as the density of the model.

Loading the Footing

After positioning and counterweighting the loading beam, the proving ring and loading column were rigidly attached. Contact was made between the loading column and the seat on the footing by lowering the loading beam. The batteries were wired across the coils and the sliding contact bracket was brought into position.

Following the manufacturer's recommended 30 minute warm-up period, the recording instrument was connected to the coils and to the proving

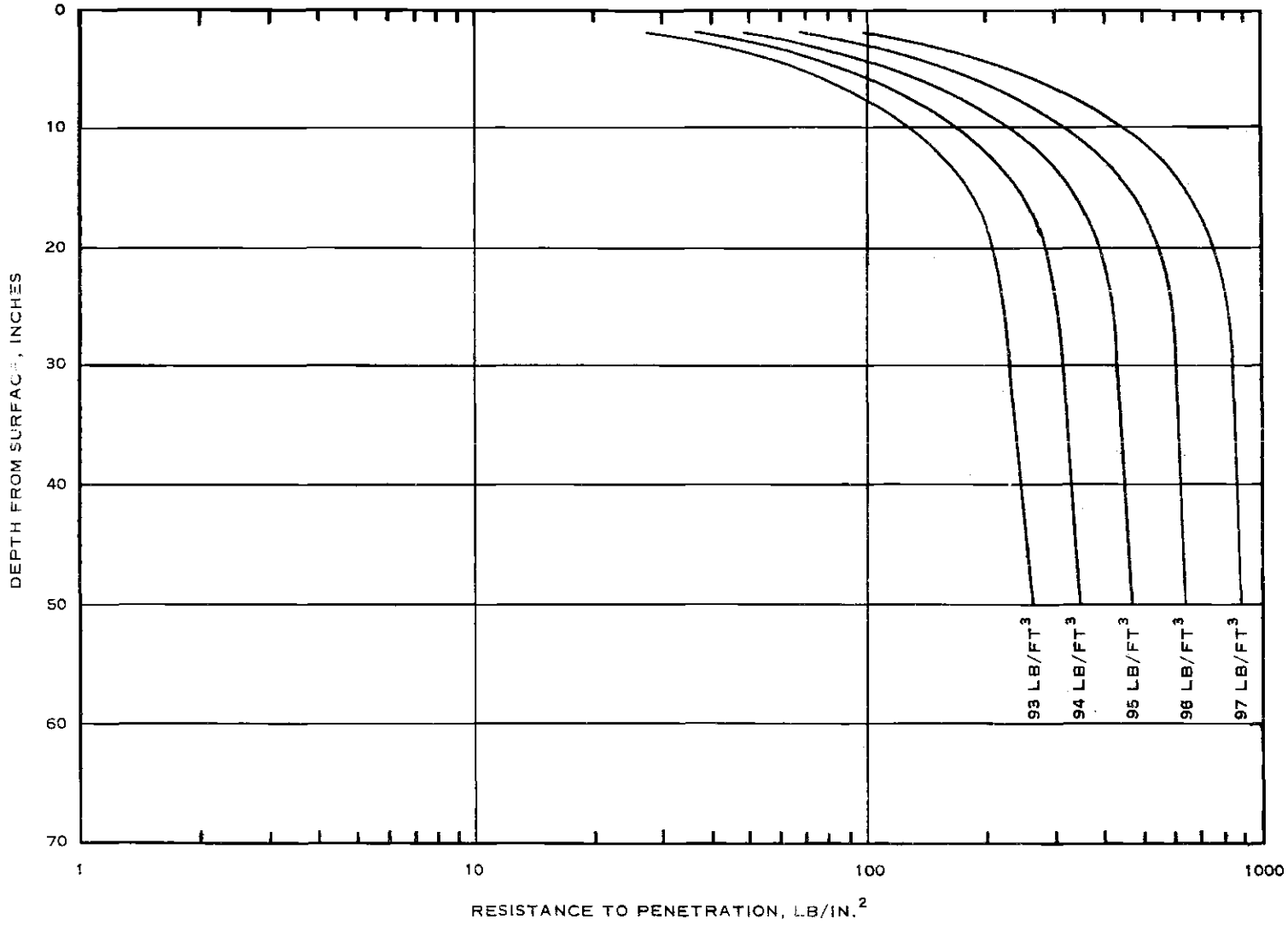

Figure 9. Penetrometer Resistance as a Function of Depth for Several Densities.

ring.

The loading head was then brought into contact with the bearing plate. A stop on the testing machine was set to limit the footing deflection to a range so that the equipment would not be damaged. From this lowered position, the head was raised at the selected loading rate for 30 seconds. From this height the testing machine would attain full velocity before again coming in contact with the bearing plate.

After starting the recording machine, the testing machine advanced downward to apply a load to the footing until the loading machine was automatically stopped.

CHAPTER III

DISCUSSION OF RESULTS

From recorded settlement-time and load-time curves, shown typically in Figure 10, the load-settlement relationship for each test could be deduced. These deduced curves all show a typical shape of an initial straight line portion which reaches a maximum load in a curve of varying degrees of curvature then turning back to a smaller load before progressing to another approximately straight line portion. See Figures 11, 12, 13, and 14.

Since the load-settlement curves all have similarity in shape the establishment of an analysis criteria was rather simple. The load at failure is the maximum load reached in the peak. The settlement at failure is the settlement corresponding to the failure load. The time to failure is the time required to obtain the failure load as determined from the recorded load-time curve. The load rate is the total settlement divided by the total time of the test.

Tests

Tests 1 through 16, with the exception of tests 13 and 15, were performed with the tripod behind the testing machine (position A). Through this lever arrangement, the loading rate applied at the footing was approximately 3 1/2 times that of the loading machine. The results obtained using this particular lever arrangement showed reasonable agreement with only nominal scattering. Tests 13 and 15 and 17 through 21 were conducted using the tripod behind the test box (position B). See

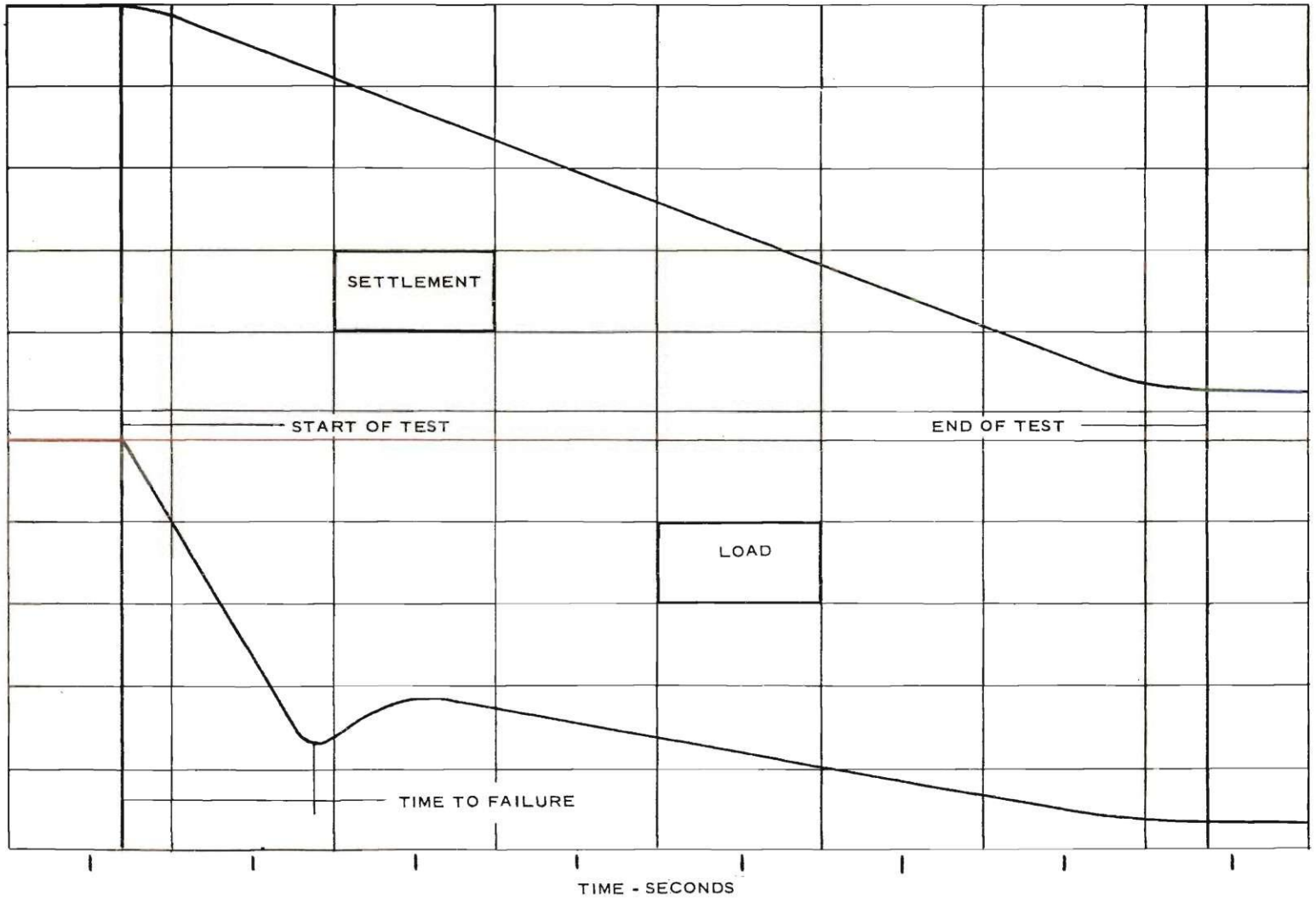

Figure 10. Typical Load-Time Curve and Settlement-Time Curve.

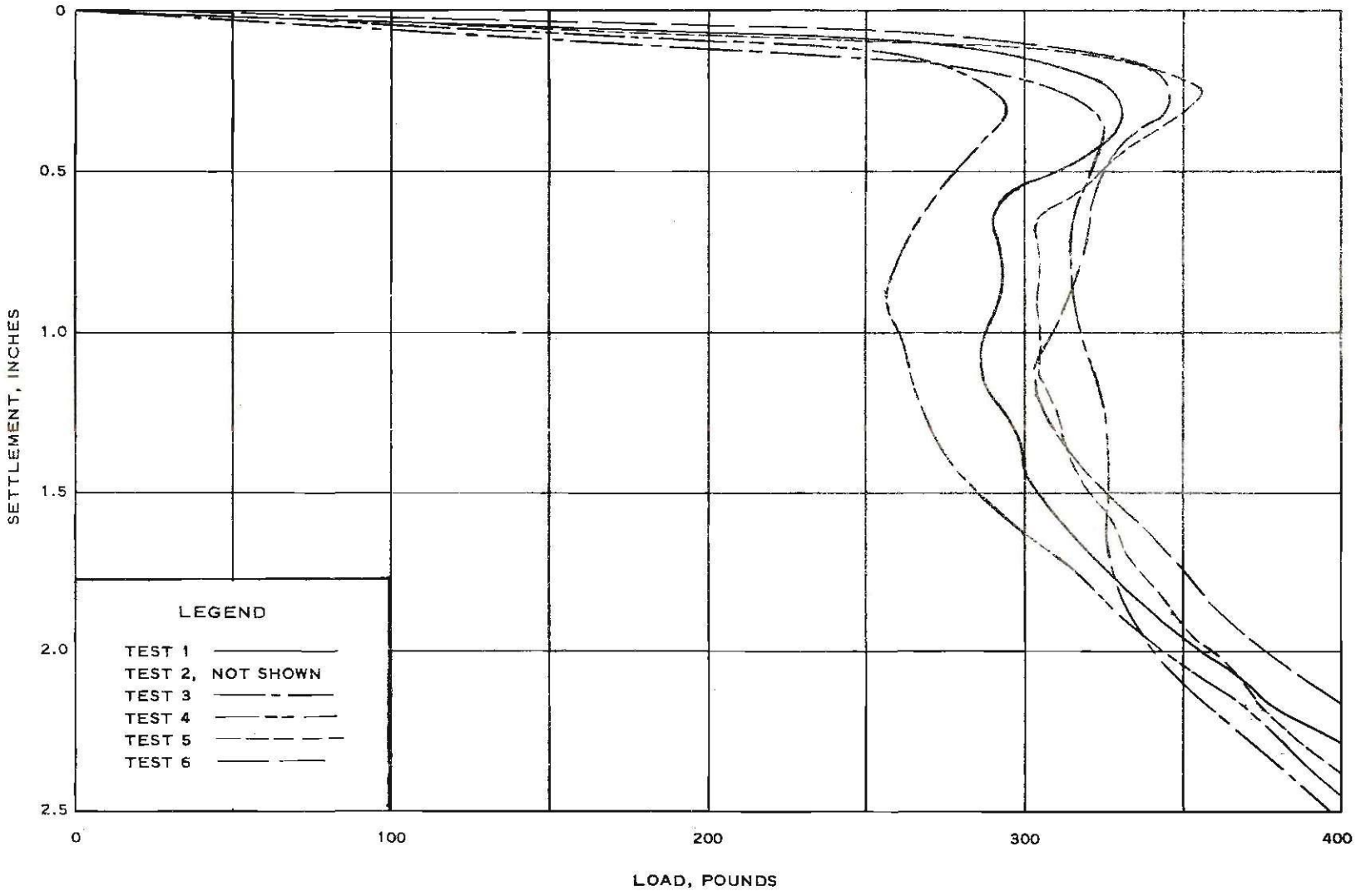

Figure 11. Load Settlement Curve (Tests 1 Through 6).

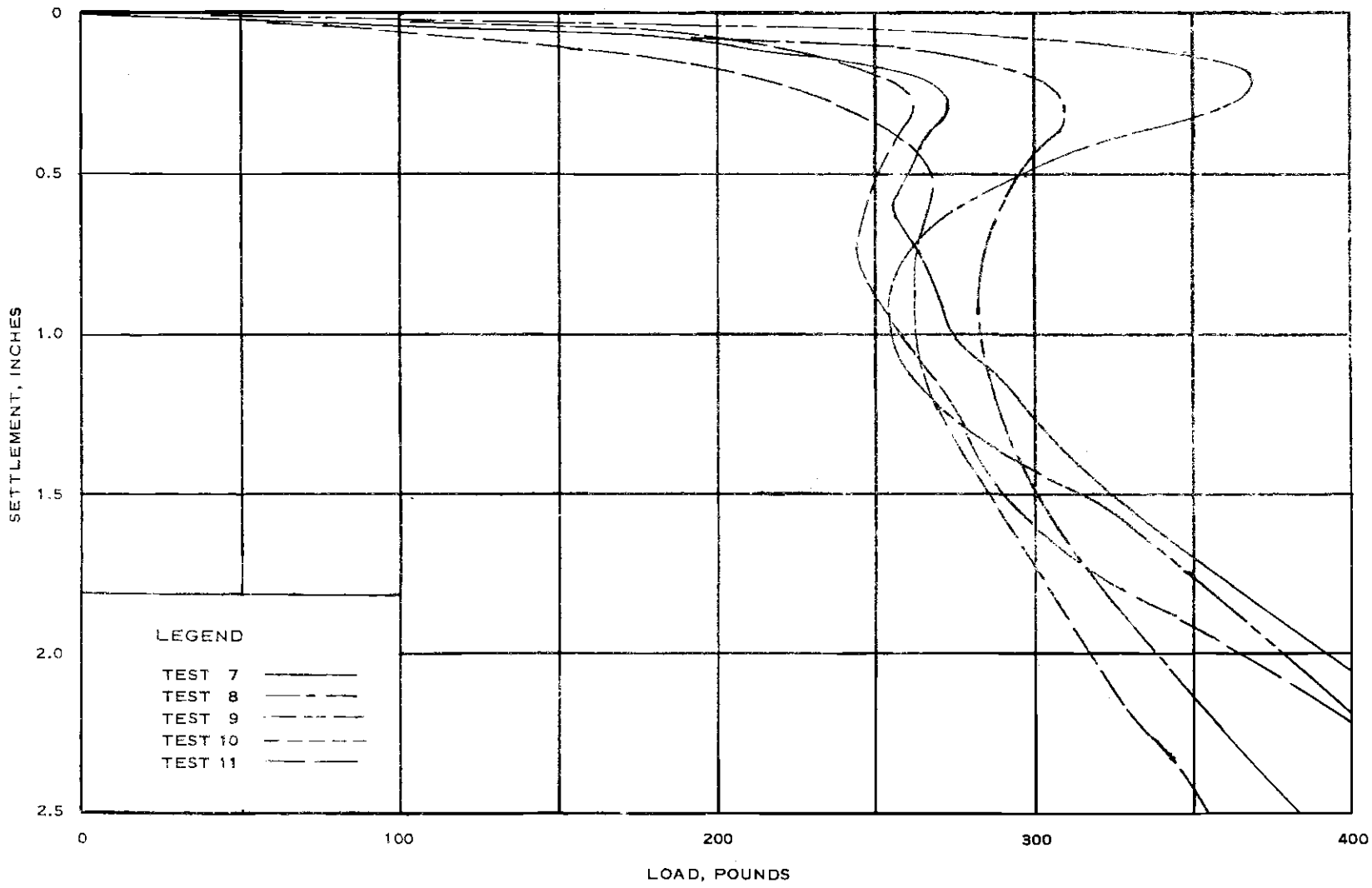

Figure 12. Load Settlement Curve (Tests 7 Through 11).

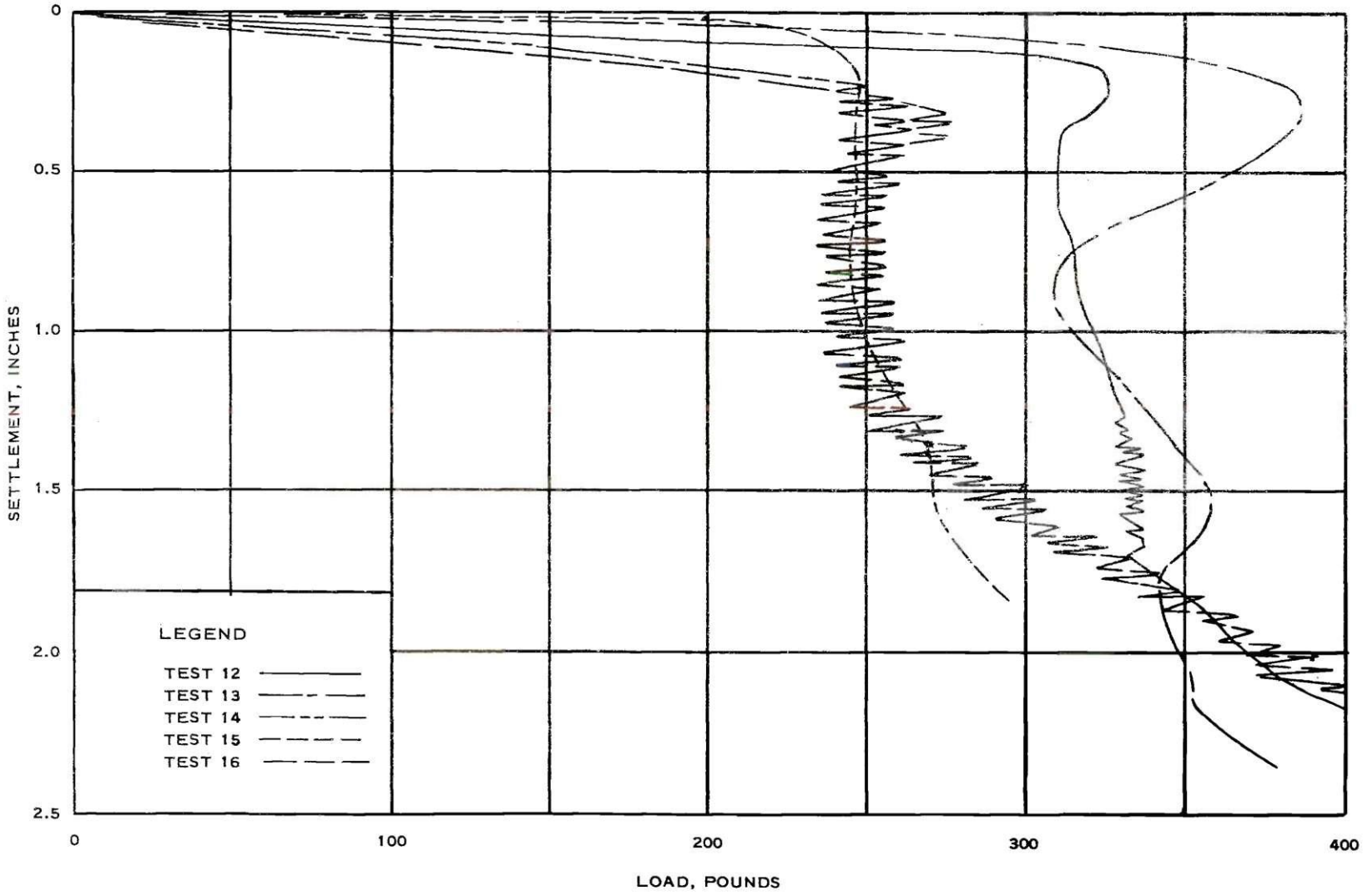

Figure 13. Load Settlement Curve (Tests 12 Through 16).

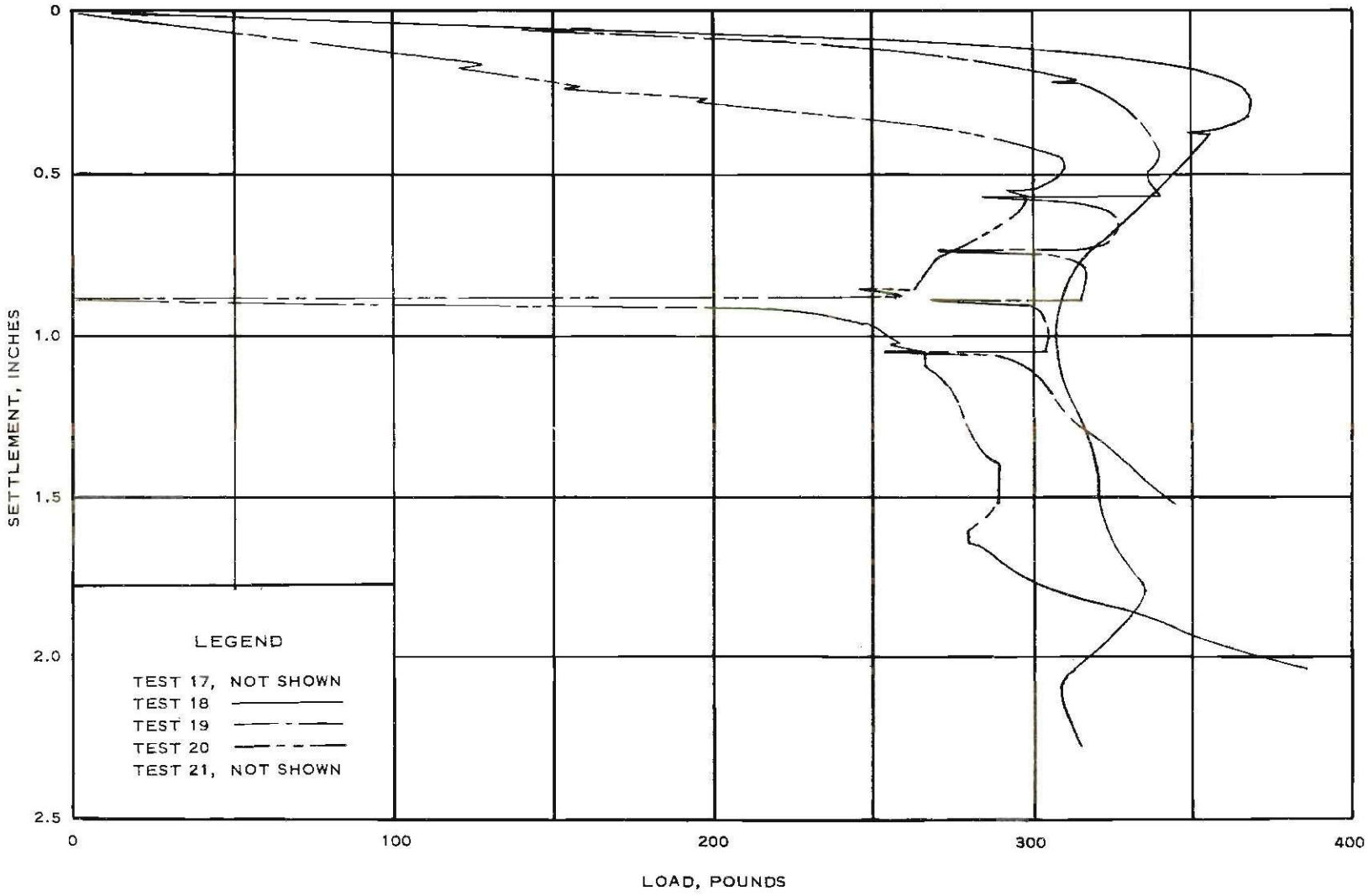

Figure 14. Load Settlement Curve (Tests 17 Through 21).

Figure 4. In this lever arrangement the loading rate at the testing machine was approximately 3 1/2 times that applied to the footing. The results of these tests were so affected by the testing arrangement that they were not comparable to the results of the tests of position A (see Appendix) and are not included in the subsequent curves and discussions.

In the summary of results, Table 1, the range of density is shown to fall between a minimum of 94.2 lb/ft^3 and a maximum of 96.8 lb/ft^3 or an increase of 2.8 per cent. Figure 2 indicates a corresponding increase in the angle of internal friction, ϕ , of 4.7 per cent from 38.0 to 39.8 degrees. For this range of variation of the angle of internal friction, the bearing capacity factors, N_γ , N_q , N_c , as indicated by Terzaghi, for example, show an increase in N_γ of 39 per cent, and increase in N_q of 29 per cent and an increase in N_c of 18 per cent.

An attempt was made to correct the data for variations in density. The data for this correction is tabulated in Table 2. Using Terzaghi's factors of N_γ , N_q , and N_c computed from the valve of ϕ for each test, a predicted value of the ultimate bearing capacity, q_{Ult} , was obtained.

By assuming that the smallest value of q_{Ult} obtained experimentally is equal that obtained theoretically it was possible to determine a value for cohesion to make the assumption correct. This value of cohesion (0.223 lb/in^2), was assumed to be a constant in all the other computations. The surcharge, q , was computed as the density of the soil mass multiplied by the settlement at failure.

Figure 15 shows the failure load as a function of the load rate, uncorrected for fluctuations in density of the sand. Figure 16 shows the

Table 1. Summary of Significant Results from Load Tests

Test	Position	Load Rate in/sec	Time to Failure sec.	Settlement at Failure in.	Load at Failure lb.	Density lb/ft^3
1	A	0.931	0.58	0.324	330	95.9
2	A	0.878	0.66	-----	360	95.7
3	A	0.842	0.71	0.349	324	95.2
4	A	0.641	1.02	0.313	293	96.3
5	A	0.500	1.3	0.228	357	95.8
6	A	0.265	2.3	0.274	345	95.6
7	A	0.120	5.1	0.274	274	95.8
8	A	0.102	6.4	0.278	310	95.5
9	A	0.0762	9.2	0.210	369	95.3
10	A	0.0283	31	0.344	266	94.2
11	A	0.0163	40	0.291	263	95.7
12	A	0.00621	100	0.212	325	96.2
13	B	0.00302	117	0.242	386	96.1
14	A	0.00090	861	0.358	264	96.8
15	B	0.00085	336	0.197	247	96.1
16	A	0.00076	894	0.306	275	95.8
17	B	0.00053	460	0.294	410	95.8
18	B	0.00052	536	0.281	368	95.8
19	B	0.00022	1604	0.437	339	96.4
20	B	0.00011	2664	0.466	311	95.8
21	B	0.00005	5364	-----	370	96.0

Table 2. Theoretical Ultimate Bearing Capacity

Compared to Experimental Ultimate Bearing Capacity

Test	ϕ	c lb/in^2	N_c	1/2 γB lb/in^2	N_γ	q lb/in^2	N_q	Theo q_{Ult} lb/in^2	Exp q_{Ult} lb/in^2	Exp/Theoret %
1	39.1	0.227	84	0.1110	102	0.0180	86	19.1	26.3	138
2	39.0		83	0.1108	100	0.0180	85	18.6	28.6	152
3	38.6		80	0.1102	94	0.0190	80	18.1	25.8	143
4	39.4		87	0.1114	109	0.0174	90	20.0	23.3	117
5	39.1		84	0.1108	102	0.0126	86	18.9	28.4	150
6	38.9		83	0.1106	99	0.0152	84	18.6	27.4	147
7	39.1		84	0.1108	102	0.0152	86	19.0	21.8	115
8	38.9		83	0.1106	99	0.0154	84	18.6	24.7	133
9	38.7		81	0.1104	96	0.0116	82	18.0	29.4	163
10	38.0		75	0.1090	84	0.0296	73	17.0	21.3	125
11	39.0		84	0.1108	100	0.0161	85	19.0	20.9	110
12	39.3		86	0.1114	106	0.0118	89	19.4	25.9	134
13	39.3		86	0.1112	106	0.0135	89	19.5	30.7	157
14	39.8		89	0.1120	115	0.0200	94	21.0	21.0	100
15	39.3		86	0.1112	106	0.0110	89	19.4	19.6	101
16	39.1		84	0.1108	102	0.0170	86	19.1	21.9	115
17	39.1		84	0.1108	102	0.0163	86	19.1	32.6	171
18	39.1		84	0.1108	102	0.0153	86	19.0	29.3	154
19	39.5		87	0.1116	110	0.0244	91	20.5	27.0	132
20	39.1		84	0.1108	102	0.0244	86	19.6	24.7	126
21	39.2		85	0.1110	104	0.0250	88	19.7	29.4	149

N_c , N_q , N_γ after Terzaghi

Shape factor 0.6

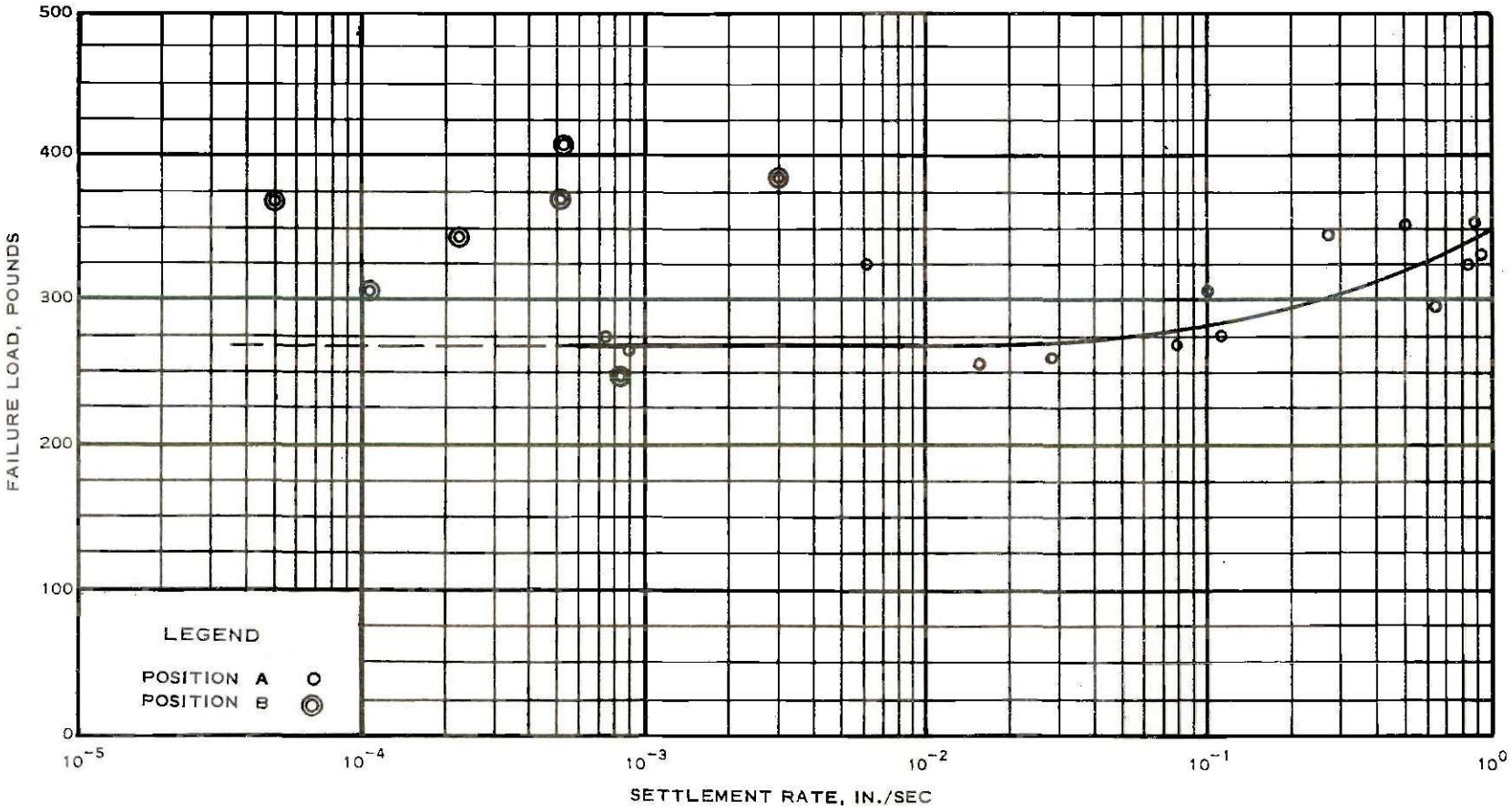

Figure 15. Failure Load as a Function of Settlement Rate.

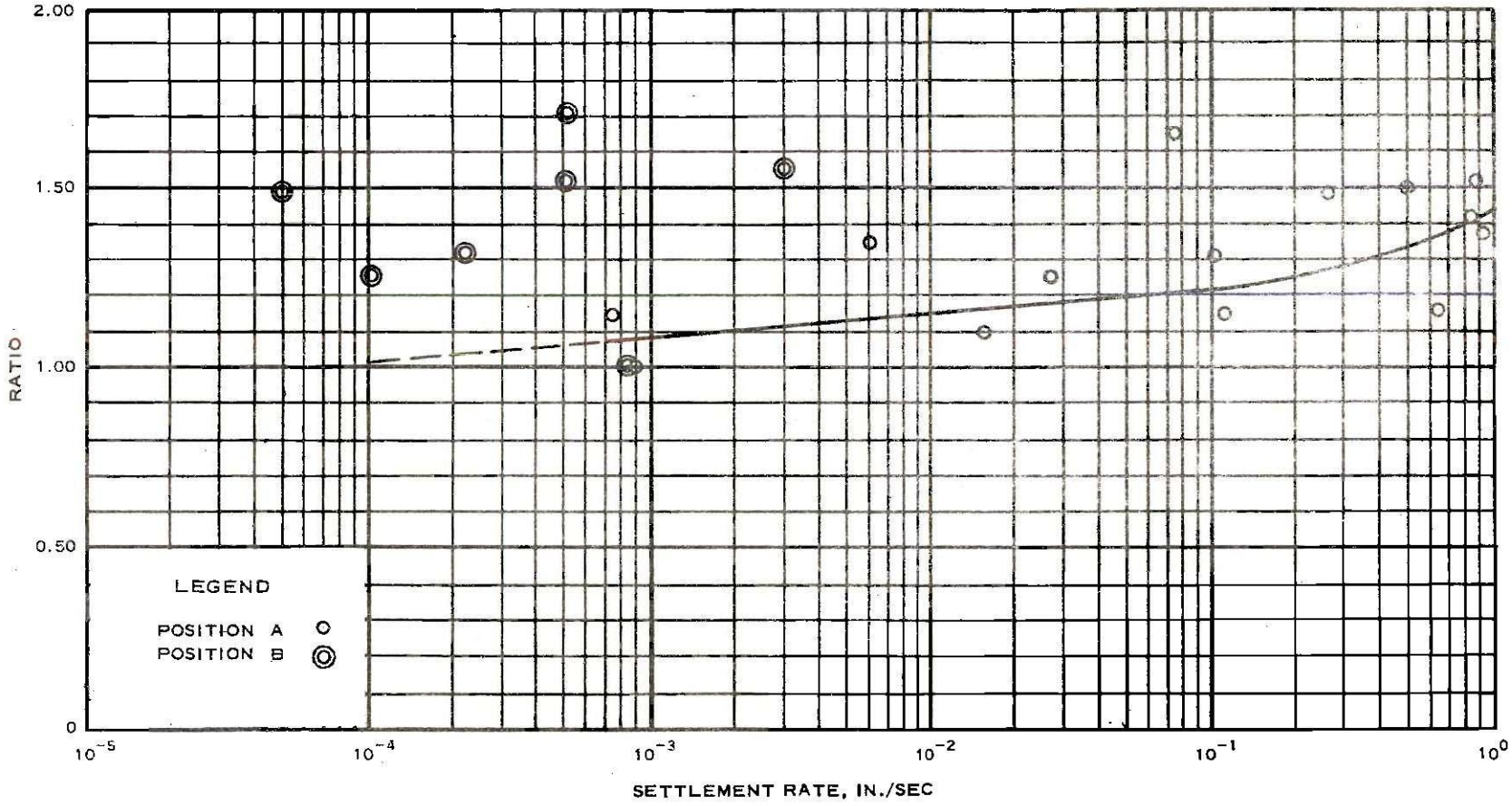

Figure 16. Ratio q_{Ult} (Experimentally)/q_{Ult} (Theoretically) as a Function of Settlement Rate.

ratio of the ultimate bearing capacity obtained experimentally to that obtained theoretically.

The resulting curves are shown to approach an asymptote at either end of the load rate spectrum. No effort was made to obtain a quantitative expression for the functions indicated.

Significant of the tests run at the slowest load rates was the behavior of the load-deflection curves. The plot of tests 14 and 16, Figure 13, shows a zigzag variation occurring. As indicated, the load would reach a peak value with continuous linear deflection whereupon there would be a sudden drop in the load and a corresponding sudden increase in the deflection. Since to each dip of the load there corresponded a sharp increase in the deflection, the phenomena is attributed to a bearing failure and not to a lateral motion of the footing. The occurance of the progressive failures was not detected in the tests of faster load rates. Although it may be argued that the time interval in which the faster tests were conducted was so short that the recording machine did not have time to record the small incremental jumps, it appears more logical to accept the explanation of the behavior of the sand at failure under kinematic conditions.

In observations by de Josselin de Jong (12) of the behavior of a pile brought to a state of failure in a sand, there existed a nonlinear relationship of settlement with respect to time after the initial load increments were applied. Rather the settlement seemed to occur in increments or steps. The pile-soil system would appear to come to an equilibrium position under a given load increment for some short time interval. Then a short increase in the settlement would be noted.

The hesitations described above are attributed to a redistribution of grain-to-grain contact forces in the sand mass. The displacements of the sand grains bring portions of the mass into a new state of equilibrium. However, the redistribution of forces in the new arrangement brings other portions of the mass into a shearing condition. After the system has undergone series of the hesitations in settlement the system will be arranged in a state of equilibrium. As the load is increased to higher valves the hesitations blend together for a condition of continual settlement with time. This state is realized whenever the applied loads are high enough to cause the system as a whole to be in a plastic condition rather than in only isolated regions.

Figure 17 indicated the relationship between the load and the time to failure of the tests. The data suggests a curve similar to a mirror image of the load-settlement rate curve. While the scattering of points is shown to be reduced only to a minor extent, the data would seem to be a method to express the tests to common basis since fluctuation in densities would tend to be reflected in the time to fail a model at a given settlement rate.

Since the initial portion of the load-settlement curve shows a straight line, indicative of a linearly deformable solid, it is possible to deduce two constants from each test. This pair of terms, apparent modulus of deformation, E' , and modulus of subgrade reaction, k , are not altogether functions of the sand as the size, shape and rigidity of the footing also affect their magnitude.

Since both constants are some linear function of the slope of the load-settlement curve they are related. Their relationship may be ex-

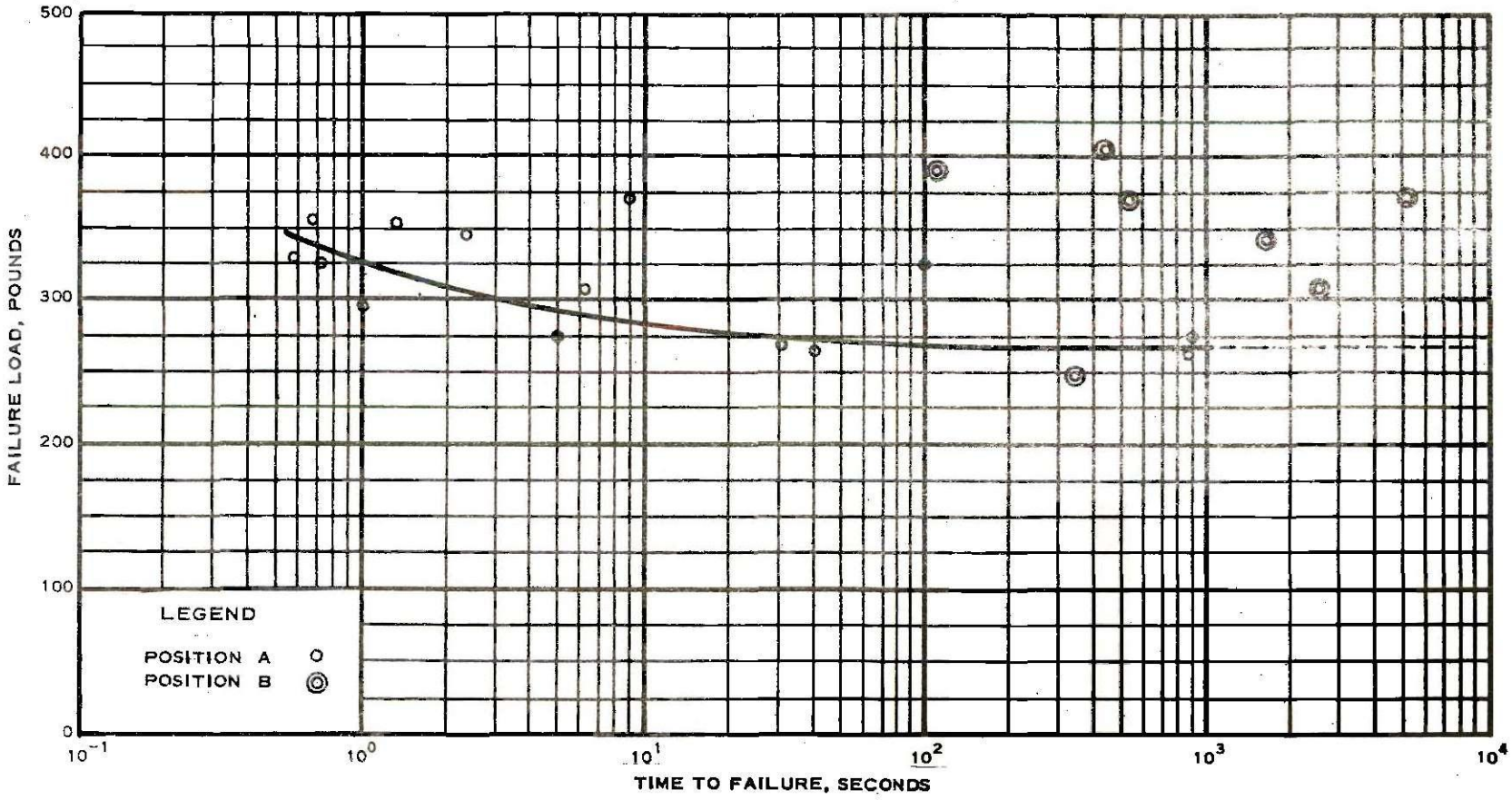

Figure 17. Failure Load as a Function of Time to Failure.

pressed as

$$E' = kBI_w$$

where

E' = apparent modulus of deformation, $E/1 - \nu^2$, lb/in^2 ,

k = modulus of subgrade reaction, lb/in^3 ,

B = footing width, inches, (4 inches for this investigation),

I_w = influence factor for settlement, dimensionless, (0.785 for a homogeneous, isotropic, elastic solid).

Figure 18 shows the variation of the modulus of subgrade reaction and apparent modulus of deformation with load rate, uncorrected for density fluctuations. Although wide scattering of data is shown a general increase (a smaller slope of the load settlement curve) is suggested as the load rate increases, indicating that the sand offers more resistance to the penetration of the footing for the fast rates of settlement.

In triaxial tests by Whitman (13) and Soteriades (14) an increase of shearing strength with an increase in the loading rate was noted in dry sands. The increase in strength observed was from 10 to 15 per cent when the time to failure was increased from that of normal triaxial tests to rates requiring only hundredths of a second for failure to occur. In this investigation, by increasing the load rate from approximately 0.001 in/sec to approximately 1.0 in/sec, an increase in the ultimate bearing capacity was 22% when uncorrected for density variations and 35% when corrected. (Figures 15 and 16). The difference in the type shear experienced in plate load tests and triaxial tests possibly accounts for the larger increase.

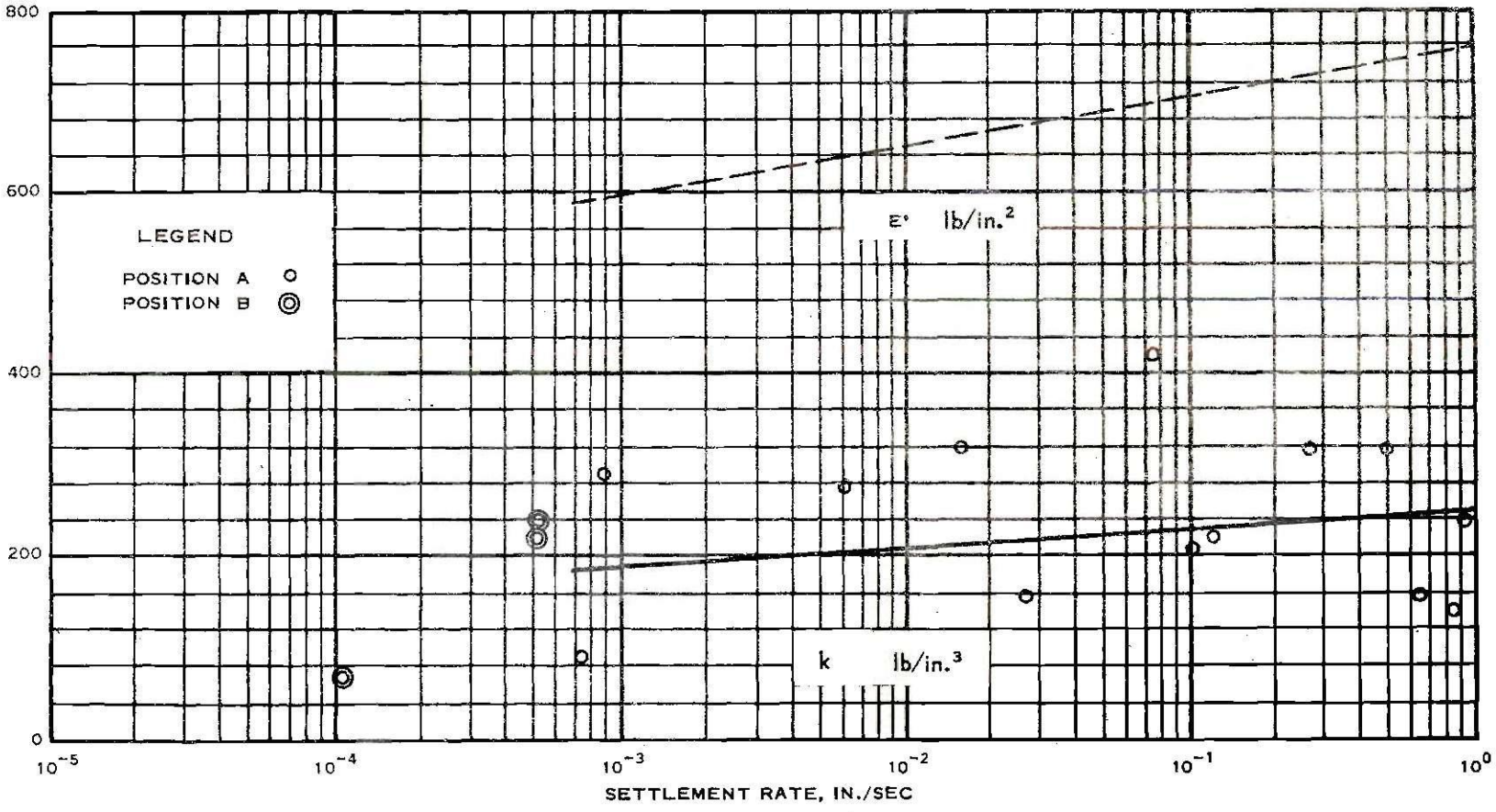

Figure 18. Apparent Modulus of Deformation and Modulus of Subgrade Reaction as a Function of Settlement Rate.

Terzaghi (15) recognized and gave an explanation to the increase in shearing resistance in his first book. Translated and summarized by Whitman (16), the shear strength increase is explained by reasoning that in rapid shear, the sand grains are not able to follow paths of less resistance and therefore shear takes place at higher values. While this explanation is plausible for shear increases in triaxial tests, it could, in principle, apply to any situation involving the shear of a soil mass.

In the general bearing capacity equation, see Appendix, by neglecting any increase in the ultimate bearing capacity, q_{Ult}, due to increases in either the cohesion, c, or the density, γ, it is easily shown that increases in the bearing capacity must result from increases in the term qN_q. This relationship may be expressed as

$$\Delta q = \gamma \, \Delta Z \quad N_q'$$

or

$$\left(\frac{\Delta q}{\Delta z}\right) \frac{1}{\gamma} = N_q'$$

As all the load settlement curves had a general increase in load after the peak load had been obtained, an average slope for the portion of the curve was computed $(\Delta q/\Delta z)$ and hence the variation of N_q' derived.

Figure 19 indicates that N_q' decreases with the faster load rates. This is to say that the resistance to the penetration of the footing after failure is higher at lower loading rates. In previous explanation, the higher failure load with the faster load rates was attributed to the sand being forced to shear without sufficient time to choose

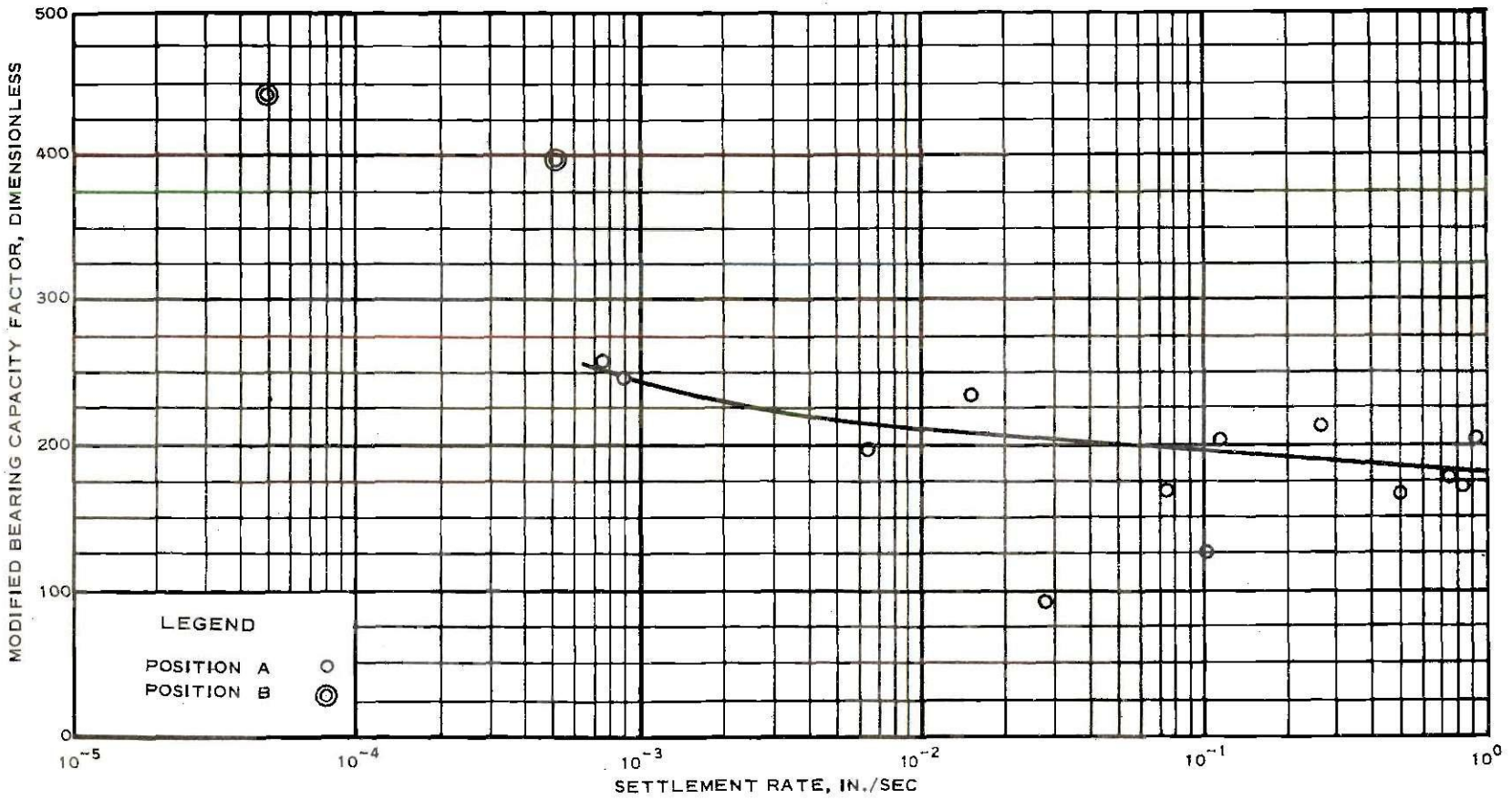

Figure 19. Modified Bearing Capacity Factor, N'_q, as a Function of Settlement Rate.

a path of least resistance. Perhaps this mechanism of failure influences a deeper but narrower zone so that as the footing is forced into the soil deeper than the settlement at failure the new shear surfaces may partially follow the old shear surfaces. It was observed that the shear surfaces tended to be at larger distances from the footing for the slow load rates (Figure 20). The same observation was also made by De Beer and Vesic (4). The conclusion of a different mode of failure occurring at the fast load rate is partially supported by observations by Selig and McKee (17). They reported a mode of failure similar to that of local shear failure in statically loaded loose sand. Multiple failure surfaces tended to associate with the tests of lower load rates, indicating new shear surfaces, hence a larger increase in resistance. See Figure 20.

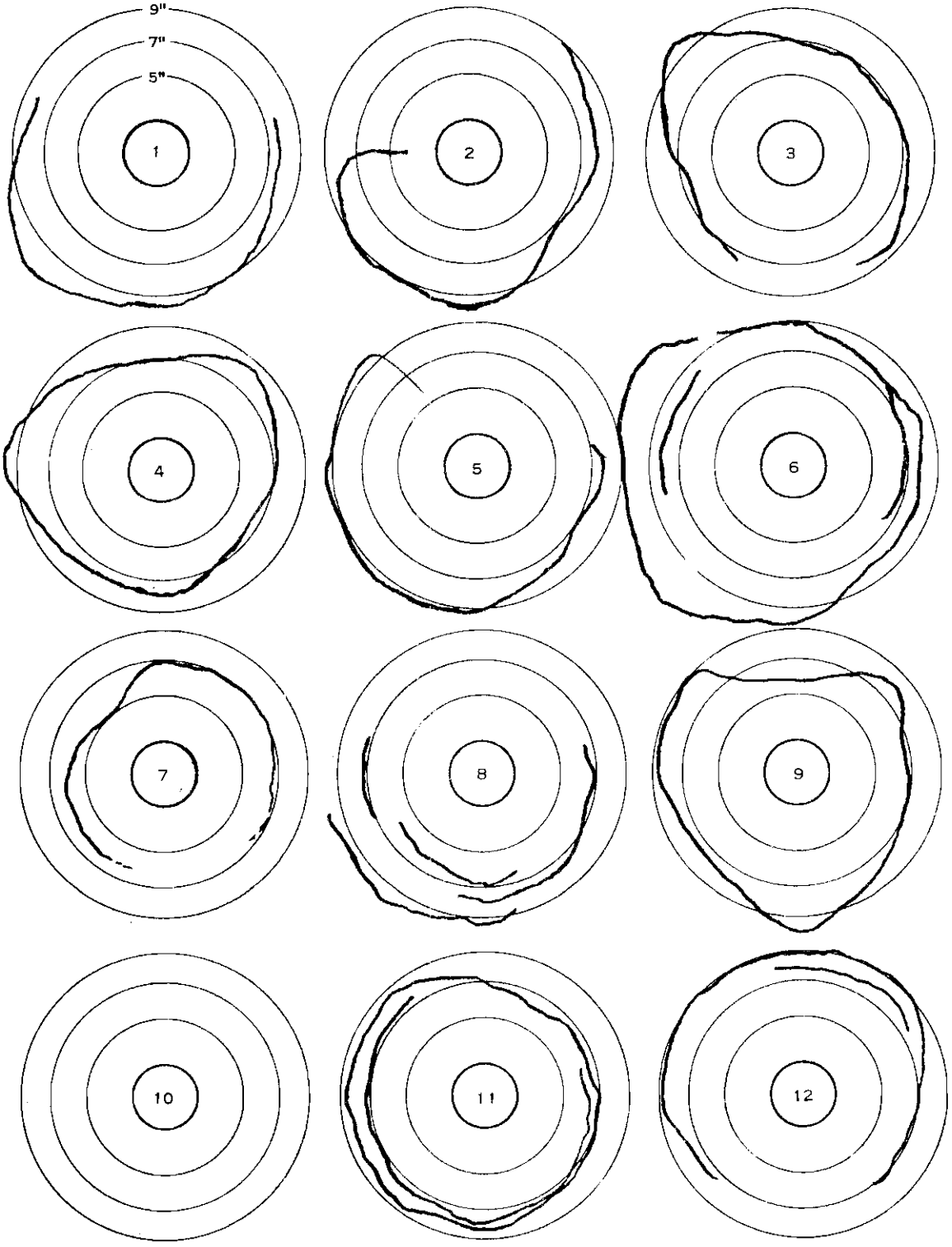

Figure 20. Shear Surfaces.

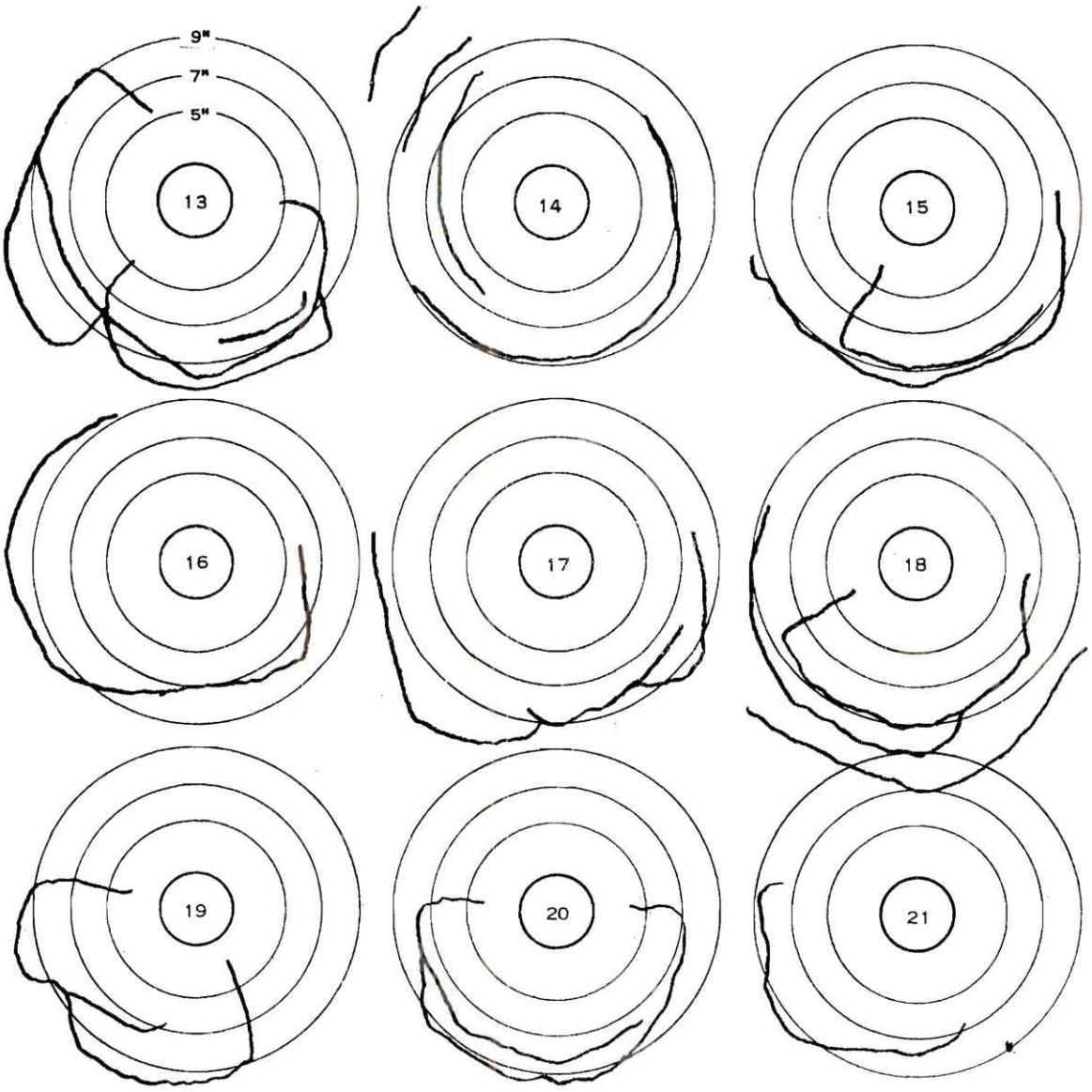

Figure 20. Shear Surfaces (Continued).

CHAPTER IV

CONCLUSIONS

Due to the high scattering of results, a considerably greater number of tests would be needed for definite conclusions. From the limited number of tests performed the following tentative conclusions may be reached:

(1) There exists an increase in the ultimate bearing capacity when a footing is forced into a sand mass at rates varying from 0.001 inches per second to 1.0 inch per second.

(2) When the footing is forced into the sand at very low rates, progressive failure occurs in the mass.

(3) A different mode of failure appears to exist in the sand at very high rates of loading.

(4) The penetration resistance seems to be greater for the models tested at low rates than for those tested at high rates.

CHAPTER V

RECOMMENDATIONS

(1) Due to scattering of results a greater number of tests should be conducted on this sand at this density.

(2) Tests should be conducted on this sand at other densities.

(3) Tests of other shapes and sizes of footings should be conducted in this sand.

(4) Preservable models should be tested to better determine the mode of failure occurring for variation in load rates.

(5) The effects of the loading system should be more carefully analyzed to correctly ascertain its contribution to the test results.

APPENDIX

NOTATIONS

a	horizontal displacement of footing (inches)
B	width of footing (inches)
c	cohesion (lb/in^2)
D	depth of base of foundation (inches)
E	modulus of deformation (lb/in^2)
E'	apparent modulus of deformation (lb/in^2)
e	void ratio
I_w	influence factor for settlement (dimensionless)
k	modulus of subgrade reaction (lb/in^3)
L	length of footing (inches)
N_c	bearing capacity factor (dimensionless)
N_q	bearing capacity factor (dimensionless)
N_γ	bearing capacity factor (dimensionless)
N'_q	modified bearing capacity factor (dimensionless)
q	surcharge (lb/in^2)
q_{Ult}	ultimate bearing capacity of a soil (lb/in^2)
Rd	relative density (dimensionless)
β	inclination of loading column from vertical (degrees)
γ	unit weight (lb/ft^3)
ν	Poisson's ratio (dimensionless)
ξ_c	shape factor in bearing capacity equation (dimensionless)
ξ_q	shape factor in bearing capacity equation (dimensionless)
ξ_γ	shape factor in bearing capacity equation (dimensionless)

$\overline{\sigma}$ effective normal stress (lb/in^2)

τ shearing stress (lb/in^2)

ϕ angle of internal friction (degrees)

GENERAL BEARING CAPACITY THEORY FOR SHALLOW FOOTINGS

Assumptions

All mathematical solutions to the bearing capacity problem have been obtained through the aid of certain simplifying assumptions. The soil mass has been assumed to be a homogeneous, isotropic, rigid-plastic material, semi-infinite in extent. The physical properties of the mass are considered to be completely defined by an evaluation of cohesion, c, angle of internal friction, ϕ, and the unit weight, γ. Furthermore, the shearing strength of the soil is assumed to be constant and defined by Coulomb's equation for failure:

$$\tau = c + \overline{\sigma} \tan \phi$$

In considering a shallow footing, the location of the base is placed so that the ratio $B/D < 1$ is satisfied. Any soil above the base is replaced with a surcharge, q, where $q = \gamma D$. The shearing resistance of the overburden is commonly neglected. The base may be either perfectly smooth or perfectly rough. The footing is considered to be long with respect to its width ($L/B > 5$). For this condition the displacements are planar rather than radical. Empirical corrections are required to define the problem of bearing capacity of circular footings, by the use of certain factors as discussed below.

Three distinct zones of rupture have been shown to exist in the soil under failure conditions. See Figure 21. Zone I is a dense, elastic zone which acts as part of the footing by moving downward during the

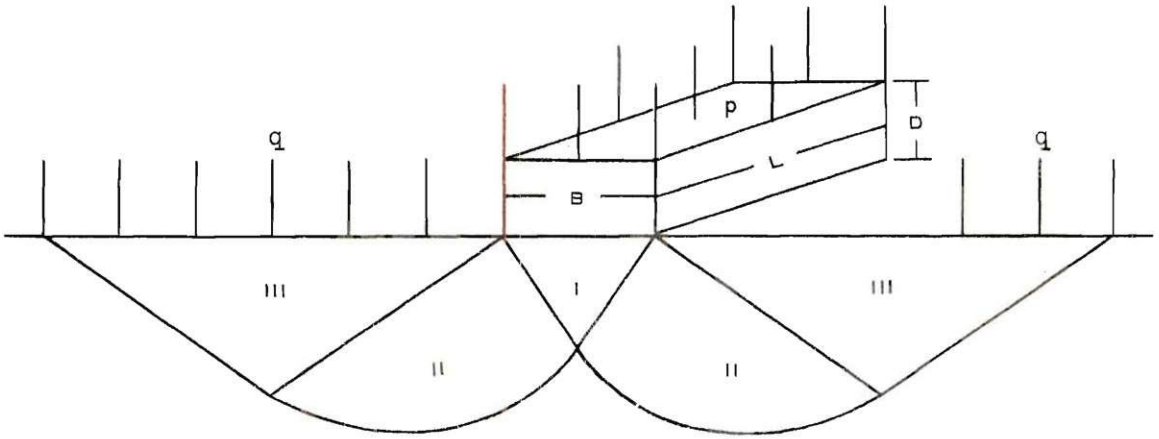

Figure 21. Shallow Bearing Capacity Problem.

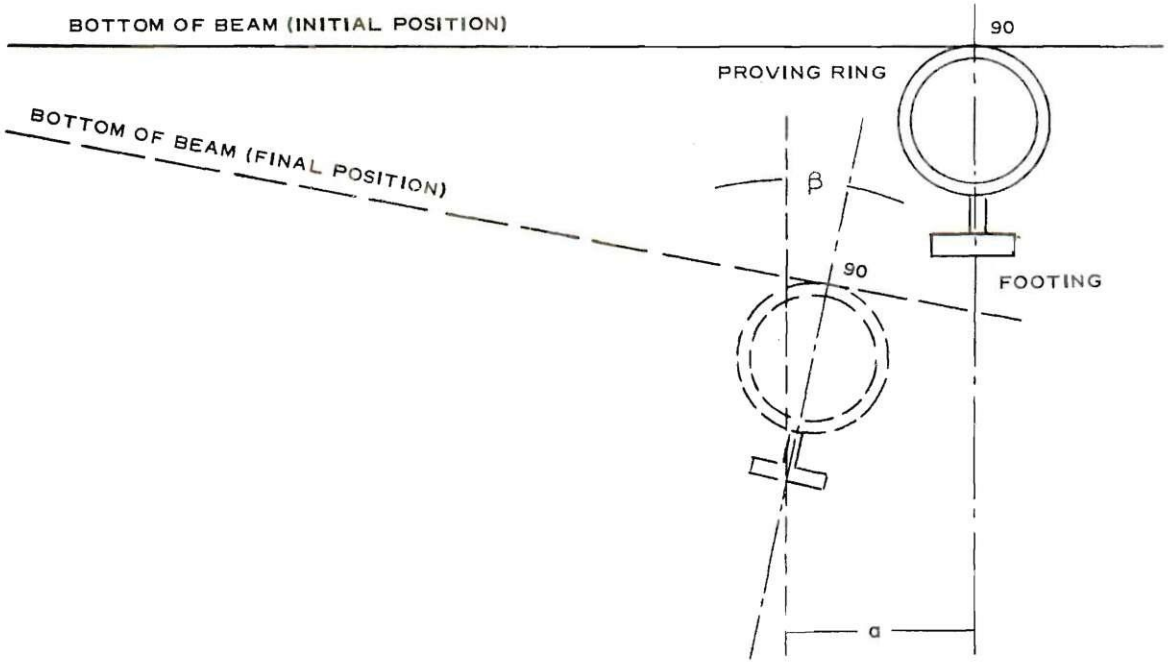

Figure 22. Changes in System During Test.

bearing capacity failure. Zone II, or Prandtl Zone, of radial shear is in the plastic state and generally moves horizontally. Zone III, or Rankine Zone, is also in a plastic condition and generally moves upward.

Solution

Although no general solution exists, certain investigators have obtained special solutions. Since many of the special solutions could be put into some form of:

$$q_{Ult} = c\, N_c + q\, N_q + \frac{1}{2}\, \gamma\, BN_\gamma$$

Terzaghi (18), among others, has suggested that the above equation could be used for the general case. In the above formula N_c, N_q, and N_γ are all dimensionless factors depending only on the value of internal friction. Model studies by De Beer and Vesic (4) have shown close agreement of the predicted values of q_{Ult} to that obtained in sands of Rd > 0.67.

Further studies to ascertain the effect of depth and shape of the footing and inclination of the footing and/or load have been conducted. These tests show that good agreement between theoretical and practical results may be obtained if the form of the general bearing capacity equation is altered to

$$q_{Ult} = c\, N_c\, \xi_c + q\, N_q\, \xi_q + \frac{1}{2}\, \gamma\, B\, N_\gamma\, \xi_\gamma$$

where ξ_c, ξ_q, and ξ_γ are dimensionless factors of the above mentioned variables.

EFFECTS OF THE LOADING SYSTEM

Tests conducted with the loading system in position B (Figure 4) were not comparable to those tests conducted for position A (Figure 3).

In the method used to record the load on the footing, the stylus deflection of the Sanborn Recorder was controlled by the change in strain of the proving ring. During all the tests there was a change in the inclination of the loading column, β, as well as a tendency for a horizontal movement of the footing, a, both of which would change the strain in the proving ring. See Figure 22. Any external effect which would change the strain in the proving ring would affect the load as deduced from the Sanborn recording. A calibration of the proving ring indicated that a horizontal load at the location of the footing would be reflected by a stylus deflection equal in magnitude to that caused by the same load acting in a vertical direction.

By the manner in which the proving ring was placed and connected to the Sanborn Recorder in tests with the tripod in position A, any horizontal load would have produced a combination of strain which would have caused a smaller stylus deflection than that which would have been caused by the vertical strain acting alone. In Tests 9 and 12 (position A) the proving ring connections were reversed so that the tendency was for the horizontal strain to be additive with the vertical strain. With the tripod in position B the horizontal strain was also additive to the vertical strain.

Table 3 shows the inclination angle, β, of the loading column

at the beginning of each test as well as the change in the angle β and the horizontal movement, a , that the footing experienced during the test. The changes in position A are seen to be small and therefore the strains, as recorded in this position, are thought to be very close to that caused by the vertical loads. In position B the changes are much more severe and affect the strains by such a magnitude that the test results could not be used for comparison in this investigation.

Further substantiating the author's decision to disregard the results of tests conducted in position B was the decrease in the time required for the footings to fail. By tracing the time to failure at comparable loading rates in Table 1 , one notices a significant decrease in the time required. This decrease is thought to be caused by the greater tendency of angular change and horizontal movement.

Table 3. Horizontal Movements and Angular Changes of Loading System During Load Test

Test	β_i min.	β_Δ min.	a_{total} in.	Position
1	10.5	58.5	0.265	A
2	0.0	54.5	0.235	A
3	21.5	53.5	0.250	A
4	3.8	47.3	0.199	A
5	14.1	47.9	0.201	A
6	18.0	47.7	0.123	A
7	19.3	44.7	0.203	A
8	14.7	46.3	0.207	A
9	5.2	43.4	0.187	A
10	12.6	45.2	0.201	A
11	23.0	43.5	0.081	A
12	10.9	43.4	0.132	A
13	70.0	154.7	0.698	B
14	7.3	52.5	0.193	A
15	90.0	120.0	0.544	B
16	22.5	42.3	0.324	A
17	11.0	166.6	0.715	B
18	29.5	151.0	0.654	B
19	65.6	101.1	0.441	B
20	20.8	130.0	0.486	B
21	8.0	83.0	0.338	B

Table 4. Load Settlement Data

Test 1 Density 95.9 lb/ft^3		Test 2 Density 95.7 lb/ft^3	
Load on Base (lb)	Settlement (inches)	Load on Base (lb)	Settlement (inches)
0	0.000	Load Data Recorded,	
90	0.029	Settlement Data Lost	
231	0.079		
296	0.144	Peak Load = 360 lb.	
326	0.231		
330	0.324		
299	0.534		
292	0.794		
286	1.15		
299	1.43		
317	1.66		
348	1.96		
381	2.19		
420	2.42		
454	2.69		
486	2.92		
517	3.13		
546	3.29		
560	3.39		

Table 4. (Continued)

Test 3 Density 95.2 lb/ft^3		Test 4 Density 96.3 lb/ft^3	
Load on Base (lb)	Settlement (inches)	Load on Base (lb)	Settlement (inches)
0	0.000	0	0.000
91	0.057	55	0.020
198	0.121	126	0.059
268	0.171	170	0.078
307	0.235	238	0.117
324	0.349	281	0.206
313	0.656	291	0.284
315	0.955	293	0.313
324	1.26	291	0.372
326	1.55	280	0.470
330	1.85	270	0.538
350	2.11	261	0.715
379	2.37	255	0.901
408	2.62	261	1.06
428	2.84	266	1.23
446	3.00	273	1.39
459	3.09	290	1.56
462	3.15	308	1.70
467	3.19	325	1.86
462	3.20	346	2.02
		366	2.16
		381	2.33
		401	2.46
		414	2.63
		425	2.75

Table 4. (Continued)

Test 5 Density 95.8 lb/ft^3		Test 6 Density 95.6 lb/ft^3	
Load on Base (lb)	Settlement (inches)	Load on Base (lb)	Settlement (inches)
0	0.000	0	0.000
40	0.045	56	0.014
121	0.063	142	0.029
193	0.072	225	0.058
255	0.091	297	0.115
312	0.145	343	0.173
349	0.208	345	0.274
357	0.253	342	0.332
350	0.326	322	0.534
335	0.416	319	0.707
313	0.593	316	0.865
304	0.706	308	1.02
305	1.17	302	1.15
312	1.32	306	1.20
325	1.56	311	1.34
336	1.76	324	1.49
351	1.95	340	1.63
369	2.13	355	1.80
389	2.31	372	1.96
413	2.47	394	2.11
439	2.69	415	2.25
453	2.83	436	2.41
		461	2.55
		482	2.68

Table 4. (Continued)

Table 7 Density 95.8 lb/ft^3		Table 8 Density 95.5 lb/ft^3	
Load on Base (lb)	Settlement (inches)	Load on Base (lb)	Settlement (inches)
0	0.000	0	0.000
56	0.029	80	0.046
129	0.043	152	0.065
196	0.101	216	0.093
251	0.159	275	0.139
265	0.202	302	0.204
274	0.274	310	0.278
270	0.346	310	0.333
261	0.518	299	0.463
256	0.612	285	0.769
264	0.727	283	1.03
270	0.879	292	1.31
276	1.01	299	1.44
293	1.16	306	1.56
304	1.30	315	1.67
317	1.45	323	1.81
338	1.59	333	1.94
355	1.73	344	2.04
370	1.85	355	2.18
391	1.99	365	2.30
411	2.13	377	2.41
432	2.27	390	2.55
445	2.40	399	2.66
468	2.62	407	2.74

Table 4. (Continued)

Test 9 Density 95.3 lb/ft^3		Test 10 Density 94.2 lb/ft^3	
Load on Base (lb)	Settlement (inches)	Load on Base (lb)	Settlement (inches)
0	0.000	0	0.000
45	0.019	34	0.032
145	0.029	86	0.048
204	0.038	148	0.112
253	0.058	207	0.192
292	0.086	246	0.320
331	0.105	265	0.448
360	0.153	268	0.544
369	0.210	265	0.640
348	0.326	263	0.817
308	0.460	262	0.897
280	0.595	263	0.993
267	0.690	265	1.15
257	0.796	276	1.33
255	0.901	286	1.50
257	1.07	297	1.67
275	1.27	308	1.86
295	1.42	320	2.02
325	1.55	331	2.19
346	1.72	343	2.32
367	1.89	355	2.50
385	2.05		
404	2.22		
417	2.39		

Table 4. (Continued)

Test 11 Density 95.7 lb/ft^3		Test 12 Density 96.2 lb/ft^3	
Load on Base (lb)	Settlement (inches)	Load on Base (lb)	Settlement (inches)
0	0.000	0	0.000
28	0.007	104	0.049
69	0.014	181	0.081
110	0.021	221	0.098
156	0.036	256	0.098
199	0.078	289	0.114
231	0.128	313	0.147
253	0.192	324	0.179
263	0.291	325	0.212
259	0.383	316	0.326
249	0.596	310	0.391
245	0.717	309	0.505
247	0.817	313	0.684
253	0.923	316	0.880
259	1.01	322	1.03
274	1.21	330	1.25
285	1.43	327	1.27
300	1.60	331	1.29
328	1.80	328	1.30
359	1.97	332	1.32
390	2.14	327	1.34
422	2.35	335	1.35
452	2.53	327	1.35
		335	1.37
		326	1.40
		336	1.42
		326	1.43
		335	1.45
		326	1.45
		335	1.47
		326	1.48
		335	1.50
		330	1.51
		335	1.51
		331	1.53
		336	1.55
		328	1.56

Table 4. (Continued)

Test 12 (continued)		Test 13 Density 96.1 lb/ft^3	
Load on Base (lb)	Settlement (inches)	Load on Base (lb)	Settlement (inches)
336	1.60	0	0.000
330	1.61	145	0.014
336	1.63	206	0.037
336	1.66	255	0.055
331	1.68	290	0.073
339	1.74	323	0.101
347	1.79	342	0.128
356	1.86	358	0.156
363	1.95	370	0.178
371	2.00	379	0.197
380	2.09	381	0.229
395	2.13	386	0.242
407	2.23	386	0.311
420	2.28	370	0.421
427	2.36	356	0.540
		327	0.654
		311	0.787
		308	0.920
		313	1.05
		334	1.24
		353	1.43
		357	1.56
		347	1.68
		341	1.82
		349	2.02
		352	2.15
		357	2.21
		368	2.28
		377	2.34

Table 4. (Continued)

Test 14 Density 96.8 lb/ft^3		Test 15 Density 96.1 lb/ft^3	
Load on Base (lb)	Settlement (inches)	Load on Base (lb)	Settlement (inches)
0	0.000	0	0.000
24	0.024	134	0.004
62	0.051	185	0.008
135	0.095	208	0.047
198	0.168	225	0.083
250	0.227	238	0.118
240	0.234	244	0.134
258	0.263	246	0.166
241	0.270	247	0.197
262	0.278	247	0.241
241	0.307	246	0.284
262	0.336	246	0.403
252	0.344	246	0.486
264	0.358	246	0.600
241	0.395	243	0.754
262	0.409	245	0.893
244	0.431	247	1.00
262	0.431	255	1.11
236	0.490	260	1.23
260	0.490	270	1.35
240	0.519	270	1.47
260	0.526	276	1.63
234	0.562	294	1.83
255	0.562		
234	0.585		
255	0.599		
234	0.636		
255	0.643		
236	0.680		
255	0.702		
233	0.716		
255	0.731		
234	0.775		
255	0.786		

Table 4. (Continued)

Test 16 Density 95.8 lb/ft^3		Test 17 Density 95.8 lb/ft^3	
Load on Base (lb)	Settlement (inches)	Load on Base (lb)	Settlement (inches)
0	0.000	0	0.000
21	0.059	116	0.034
41	0.059	192	0.068
70	0.071	180	0.068
98	0.082	199	0.075
130	0.141	291	0.109
159	0.141	348	0.164
190	0.177	384	0.198
219	0.224	401	0.246
242	0.236	410	0.294
261	0.283	409	0.328
275	0.306	398	0.417
257	0.330	366	0.588
276	0.330	346	0.807
254	0.365	338	0.937
275	0.377	326	1.08
250	0.412	329	1.20
267	0.424	335	1.37
245	0.436	325	1.37
263	0.448	331	1.37
242	0.483	335	1.46
262	0.495	328	1.46
244	0.518	334	1.47
262	0.518	336	1.58
238	0.542	340	1.68
254	0.542	345	1.81
238	0.554	350	1.98
254	0.565	370	2.04
232	0.601	391	2.15
253	0.613	415	2.26
236	0.636	439	2.35
253	0.636	462	2.43
231	0.660	490	2.51
251	0.660	505	2.55
232	0.680		

Table 4. (Continued)

Test 18 Density 95.8 lb/ft^3		Test 19 Density 96.4 lb/ft^3	
Load on Base (lb)	Settlement (inches)	Load on Base (lb)	Settlement (inches)
0	0.000	0	0.000
260	0.093	134	0.046
298	0.131	187	0.078
355	0.194	247	0.131
368	0.281	290	0.183
356	0.375	315	0.241
349	0.375	306	0.241
355	0.381	315	0.245
333	0.600	327	0.297
310	0.838	335	0.368
308	1.09	339	0.437
318	1.31	335	0.509
321	1.55	330	0.574
336	1.79	284	0.574
308	2.09	317	0.581
316	2.28	327	0.668
		319	0.733
		271	0.733
		305	0.736
		317	0.811
		315	0.896
		268	0.896
		300	0.899
		305	0.987
		304	1.05
		260	1.05
		292	1.06
		304	1.14
		306	1.22
		317	1.29
		328	1.38
		340	1.47
		344	1.52

Table 4. (Continued)

Test 20 Density 95.8 lb/ft^3		Test 21 Density 96.0 lb/ft^3	
Load on Base (lb)	Settlement (inches)	Load on Base (lb)	Settlement (inches)
0	0.000	Load Data Recorded,	
21	0.036	Settlement Data Lost	
85	0.104		
128	0.161	Peak Load = 370 lb.	
121	0.166		
148	0.207		
158	0.228		
154	0.228		
198	0.269		
195	0.269		
241	0.321		
267	0.347		
286	0.389		
300	0.404		
304	0.430		
311	0.466		
311	0.487		
308	0.502		
304	0.523		
302	0.539		
292	0.539		
300	0.544		
300	0.570		
298	0.611		
290	0.648		
288	0.658		
280	0.710		
276	0.730		
269	0.767		
267	0.803		
265	0.818		
264	0.839		
263	0.850		
247	0.850		

BIBLIOGRAPHY

1. Casagrande, A., and W. L. Shannon, "Research on Stress-Deformation and Strength Characteristics of Soils and Soft Rock Under Transient Loading," Harvard University Graduate School of Engineering Publications, No. 447, Soil Mechanics Series, No. 31, 1948.

2. Whitman, Robert V., "Testing Soils with Transient Loads," Conference on Soils for Engineering Purposes, National University, Mexico, ASTM Special Technical Publication No. 232, Philadelphia, 1957.

3. Whitman, Robert V., "The Behavior of Soils Under Transient Loading," Proceedings of the Fourth International Conference on Soil Mechanics and Foundation Engineering, Butterworths Scientific Publications, London, 1958, Vol. 1, p. 207.

4. De Beer, E. E., and A. B. Vesic, "Etude experimentale de la capacite' portante du sable sous des foundations directes 'etablies en surface," Annales des Travaux Publics de Belgique, 3, (1958), pp. 50-51.

5. Shenkman, S., and K. E. McKee, "Bearing Capacities of Dynamically Loaded Footings," Symposium on Soil Dynamics, ASTM Special Technical Publication No. 305, Philadelphia, 1961, p. 78.

6. Cunny, R. W., and R. C. Sloan, "Dynamic Loading Machine and Results of Preliminary Small-Scale Footing Tests," Symposium on Soil Dynamics, ASTM Special Technical Publication No. 305, Philadelphia, 1961, p. 65.

7. Selig, E. T., and K. E. McKee, "Static and Dynamic Behavior of Small Footings," Journal of the Soil Mechanics and Foundations Division, Proceedings of the American Society of Civil Engineers, Vol. 87, No. SM6, Pt. 1, December, 1961, p. 29.

8. Cunny, R. W., and R. C. Sloan, "Static and Dynamic Behavior of Small Footings (Discussion of)," Journal of the Soil Mechanics and Foundation Division, Proceedings of the American Society of Civil Engineers, Vol. 88, No. SM4, Pt. 1, August, 1962, p. 200.

9. Shenkman, S., and K. E. McKee, op. cit., p. 78.

10. Duncan, J. M., The Influence of Depth on the Bearing Capacity of Strip Footings in Sand, Unpublished Master's Thesis, Georgia Institute of Technology, 1962.

11. Kluge, R. W., "Proving-Ring Design Chart," Engineering News-Record, December 7, 1939, p. 94.

12. de Josselin de Jong, G., "Statics and Kinematics in the Failable Zone of a Granular Material," Delft, Uitgererij Waltman, Proefschrift, Technische Hogeschool te Delft, 1959.

13. Whitman, Robert V., "Testing Soils," p. 245.

14. Soteriades, M., Stress-Strain-Time Phenomena in Sands Under Triaxial Testing Conditions, Unpublished Master's Thesis, Massachusetts Institute of Technology, 1954.

15. Terzaghi, Karl, Erdbaumechnik, Franz Deuticke, Leipzig and Wien, 1925, p. 101.

16. Whitman, Robert V., "Testing Soils," p. 245.

17. Selig, E. T., and K. E. McKee, op. cit., p. 46.

18. Terzaghi, Karl, Theoretical Soil Mechanics, 1st ed., New York, John Wiley and Sons, Inc., 1943, p. 125.